Role of Ion Exchange in Solid-State Chemistry

ABRAHAM CLEARFIELD

Department of Chemistry, Texas A&M University, College Station, Texas 77843

Contents

Abraham Clearfield was born in Philadelphia and received a B.A. and M.A. in Chemistry from Temple University. His Ph.D. degree was earned at Rutgers University and conferred in 1954. He served as a chemist with the U.S. Army Quartermaster Corp and was employed from 1955 to 1963 by the National Lead Co. (NL Industries). He joined the faculty of Ohio University in Athens, Ohio, in 1963 and became a full professor in 1968. He served as a program director for Thermodynamics and Structure at the National Science Foundation during 1974–1975 and as Chaiman of the Solid State Subdivision of the American Chemical Society in 1986. He joined the faculty of Texas A&M University in 1976. He is currently Associate Dean for Research of the College of Science and Director of the Texas A&M University Materials Science Program. He has published over 160 papers in the areas of crystallography, solid-state chemistry, and inorganic ion exchange materials, and has won awards for excellence in teaching and research.

I. Introduction

A. Background

Until recently, ion exchange behavior was thought to be confined to a very limited number of inorganic compound types. Among these the best known are the clays and zeolites, both natural and synthetic. However, as work progressed in this area, it has come to be recognized that ion exchange properties are possessed by many different classes of compounds.[1-3] A partial listing of such compound types is presented in Table 1. A discussion encompassing all these classes of compounds would require the preparation of a series of books. Therefore, our intention is to limit the scope here to those aspects of inorganic ion exchange which are relevant to solid-state chemistry. The topics covered will include synthesis of new exchangers and examination of their properties, the use of ion exchange

TABLE 1. Principal Classes of Inorganic Ion Exchangers

type	example	exchange capacity, mequiv/g
1. smectite clays	montmorillonites $M_{x/n}{}^{n+}[Al_{4-x}Mg_x](Si_8)O_{20}(OH)_4$	0.5–1.5
2. zeolites	$Na_x(AlO_2)_x(SiO_2)_y \cdot zH_2O$	3–7
3. substituted aluminum phosphates	silicoaluminophosphates, metal-substituted aluminophosphates $(M_x{}^{n+}Al_{1-x}O_2)(PO_2)(OH)_{2x/n}$	depends upon value of x
4. hydrous oxides	(a) $SiO_2 \cdot xH_2O$, $ZrO_2 \cdot xH_2O$	1–2
	(b) $(H_3O)_2Sb_2O_6$, polyantimonic acid	2–5
5. group IV (groups 4 and 14[a]) phosphates	$Zr(HPO_4)_2 \cdot H_2O$, $Sn(HPO_4)_2 \cdot H_2O$	4–8
6. other phosphates	uranium phosphates, vanadium phosphates, antimony phosphates	
7. condensed phosphates	$NaPO_3$	$\simeq 8$
8. heteropolyacid salts	$M_nXY_{12}O_{40} \cdot xH_iO$ (M = H, Na$^+$, NH$_4{}^+$; X = P, As, Ge, Si, B; Y = Mo, W)	0.2–1.5
9. ferrocyanides	$M_{4/n}{}^{n+}Fe(CN)_6$ (M = Ag$^+$, Zn^{2+}, Cu^{2+}, Zr^{4+}; n = ion charge)	1.1–6.1
10. titanates	$Na_2Ti_nO_{2n+1}$ (n = 2–10)	2–9
11. apatites	$Ca_{10-x}H_x(PO_4)_6(OH)_{2-x}$	cation and anion exchange
12. anion exchangers	hydrotalcite	anion exchange
	$Mg_6Al_2(OH)_{16}CO_3 \cdot 4H_2O$	2–4
13. miscellaneous types	alkaline-earth sulfates, polyvanadates, sulfides	
14. fast ion conductors	β-alumina, $Na_{1+x}Al_{11}O_{17+x/2}$	1.5–3
	NASICON, $Na_{1+x}Zr_2Si_xP_{3-x}O_{12}$	2–7

[a] In this paper the periodic group notation in parentheses is in accord with recent actions by IUPAC and ACS nomenclature committees. A and B notation is eliminated because of wide confusion. Groups IA and IIA become groups 1 and 2. The d-transition elements comprise groups 3 through 12, and the p-block elements comprise groups 13–18. (Note that the former Roman number designation is preserved in the last digit of the new numbering: e.g., III → 3 and 13.)

processes to synthesize new compounds, proton and fast ion transport, electrochemical devices based on ionic conductors, and some theoretical considerations. As far as possible we shall try to describe in structural terms the underlying basis for the observed behaviors and related structure to synthetic processes. In addition to the limitations listed above, we shall also not discuss zeolites and clay chemistry as these subjects are adequately treated in the literature.[4-9]

B. A Brief History

Ion exchange was originally discovered to take place in soils by Thompson[10] and by Way and Roy.[11] The active compounds were later identified by Lemberg[12] and by Wiegner[13] to be clays, glauconites, zeolites, and humic acids. It was not until the beginning of the 20th century that this knowledge was applied to the development of water softeners. The first commercially available ion exchangers were amorphous aluminosilicate gels.[14,15] These gels later become known as permutites but their instability toward acid solutions and variability of behavior led chemists to seek alternatives. This search eventually led to the synthesis of organic ion exchange resins.[16] These resins soon dominated the field because of their uniformity, chemical stability, and the ability to control resin properties by synthetic procedures. This situation existed until the post World War II era. The advent of nuclear technology initiated a search for ion exchange materials that would remain stable above 150 °C and in high radiation fields. Early attention was focused on hydrous oxides since it was known that they "sorbed" or coprecipitated many ions. It was soon discovered that hydrous oxides combined with anions such as phosphates, vanadates, molybdates, and antimonates produced superior ion exchangers.[17-20] Much attention was paid to the synthesis and properties of zirconium phosphate, which actually had been discovered earlier[21] but remained hidden as a classified document. These materials were amorphous in nature and not resistant to alkaline hydrolysis. In fact, extensive hydrolysis occurred even in hot water. Therefore, they were never extensively utilized. The exception was the use of amorphous zirconium phosphate as a sorbant in portable artificial kidney devices.[22]

A new direction was applied to the field of inorganic ion exchangers when Clearfield and Stynes[23] demonstrated that zirconium phosphate could be crystallized. The availability of crystals allowed the structure of this polymorph of zirconium phosphate to be determined,[24-27] and with this knowledge, the observed ion exchanger behavior could be explained in structural terms.[1]

Paralleling the progress in the field of nonsilicate ion exchangers, rapid developments were taking place in zeolite chemistry. The brilliant research of Barrer and his co-workers[28] finally led to the synthesis of the faujesite family of zeolites by Union Carbide scientists.[29] However, the rapid growth of zeolite technology not only stemmed from their use as sorbants and ion exchangers, but also as catalysts, particularly in petroleum cracking.[30] Zeolite chemistry in all its aspects has continued to expand, and many new and startling discoveries have been made in recent years.[31,32] Zeolites and molecular sieves exhibit such complex behavior that continued research will undoubtedly lead to new discoveries and technology. An interesting facet of their technology pertinent to our discussion is the recent use of zeolite-A as a water softener in certain detergents. The tonnage now consumed is larger than that of all the organic resins combined.

While the original intent of the studies in hydrous oxides and salts of polyvalent acids was the exploration of their ion exchange properties for separations and removal of ions from nuclear waste streams, our increased knowledge of these behaviors needs to be applied in order to properly describe the solid-state chemistry of many of these compounds. We shall begin by describing how these concepts apply to the hydrous
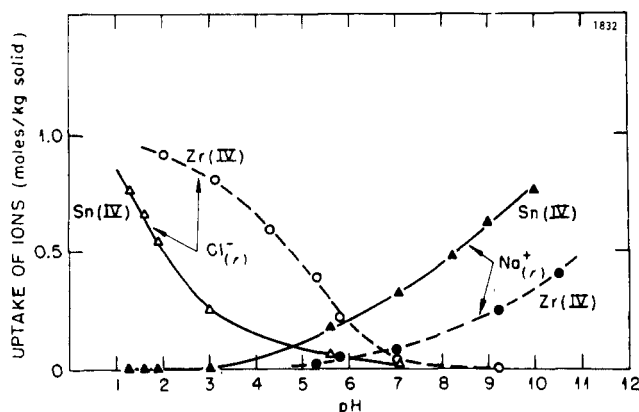
Figure 1. Ion exchange capacity versus pH for hydrous tin and zirconium oxides. (From ref 18, with permission.)

oxides and how new compounds may be synthesized and characterized on this basis.
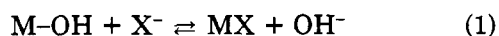
II. Hydrous Oxides

The hydrous oxides may be divided into two main types: those like ZrO_2 and SnO_2 for which ion exchange occurs only on the surface, and others such as the hydrous oxides of antimony and manganese, which contain cavities or tunnels in which exchangeable ions reside. The former compounds have been termed particle hydrates while the latter are referred to as framework hydrates.[33]

A. Particle Hydrates

1. Structural and Ion Exchange Description

All of the group III (groups 3 and 13; see footnote a in Table 1 for more on this group notation) and group IV (groups 4 and 14) metals produce hydrous oxides that belong to this class. They are usually prepared by the addition of base to a soluble salt of the cations. Polyvalent cations hydrolyze in water, and as hydroxyl groups accumulate on the cation through hydrolysis or base addition, they polymerize by olation.[34] When the olation process produces sufficiently large particles of reduced charge, precipitation occurs. Rapid precipitation in the cold leads to amorphous or poorly crystalline products, whereas aging, boiling, or hydrothermal procedures yield crystalline hydrous oxides.[34,35] The X-ray diffraction patterns of the crystalline hydrous oxides resemble the same crystalline oxides formed by high-temperature reactions. For example, TiO_2 forms anatase or rutile while hydrous ZrO_2 can be prepared in both monoclinic and cubic forms.[35] Unit cell dimensions determined for these crystalline hydrous oxides are not too different from those of the calcined oxides. Thus, the structure of the interiors of the hydrous oxides must closely resemble that of the calcined oxides with all the hydroxyls and water molecules on the surface.

The surface groups are responsible for the observed ion exchange behavior. These hydrous oxides can function as both cation and anion exchangers. This amphiprotic behavior arises as follows:

$$M-OH + X^- \rightleftharpoons MX + OH^- \qquad (1)$$

$$M-OH + A^+ \rightleftharpoons MOA + H^+ \qquad (2)$$

Process 1 takes place more readily in acid solution whereas reaction 2 is more prevalent in alkaline solu-
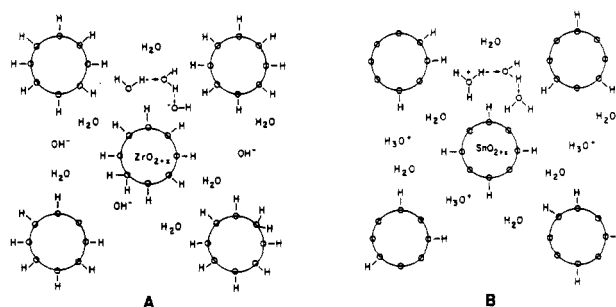

Figure 2. Schematic representation of hydrous oxide particles. (A) $ZrO_2 \cdot nH_2O$ with hydroxyl ion in the intercrystalline water neutralizing the positively charged particle surface. (B) $Sn_2O \cdot nH_2O$ with H_3O^+ in the intercrystalline water neutralizing the negatively charged particle surface. (From ref 33, with permission.)

tion. In Figure 1 are shown ion uptake curves as a function of pH for hydrous tin and zirconium oxides.[18] We note that tin oxide, being more acidic than ZrO_2, exchanges more cations at the same pH than does ZrO_2. The opposite is true for anion exchange. These phenomena are general. For example, hydrous silica or silicic acid is so acidic that it exhibits few, or no, anion exchange properties. The point at which the cation and anion curves cross is called the zero point of charge (ZPC) and represents a region in which the charge on the surface is zero. The pH at which this occurs for any given oxide is not constant but depends upon the preparative conditions, crystallinity, and degree of aging.[36,37]

A simple but more quantitative structural model of hydrous oxides has recently been proposed.[33] The description of hydrous zirconia and how it forms by olation followed by oxolation is essentially that presented by Clearfield.[35,38-40] The hydrous oxide interior is considered to be a dense, anhydrous oxide. Within the ZrO_2 particle, each Zr^{4+} ion is surrounded by eight oxygen atoms (fluorite structure) while each oxygen is in turn coordinated by four metal atoms. The situation on the surface is quite different. Here the oxygen atoms are all associated with protons, either as hydroxyl groups or as water molecules, because the process of oxolation and particle condensation is incomplete. Terminal oxygens are thought to belong to water molecules and bridging oxygen to hydroxyls. This proton association makes the clusters positively charged. The assumption is made that all the metal atoms at the surface retain the full oxygen coordination of the interior, which results in an O/Zr ratio, R, greater than 2, since the surface oxygens are not fully coordinated to metal atoms. The authors[33] calculate R to be 2.6 for a cubic-fluorite particle of 25 Å and 2.15 for a 100-Å particle. Individual particles are closely associated to form the hydrous oxide gel in which water molecules fill the voids between particles. This interparticle solution, S, is either acidic (S_A) or basic (S_B), depending upon the degree of protonation at the particle surface. A schematic representation of this model for both ZrO_2 and SnO_2 is given in Figure 2.

According to England et al.,[33] hydrous tin oxide produces a weakly acidic solution when equilibrated with water. This indicates that the surface is negatively charged by dissociation of hydroxyl groups to form O^{2-} as shown in eq 3. The liberated protons then reside
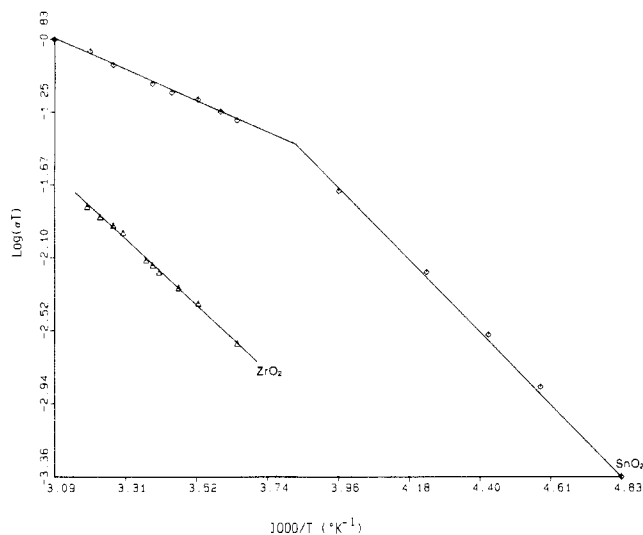
$$M-OH + H_2O \rightleftharpoons MO^- + H_3O^+ \qquad (3)$$

Figure 3. log (σT) versus reciprocal temperature for $SnO_2 \cdot nH_2O$ and $ZrO_2 \cdot nH_2O$. (From ref 33, with permission.)

in the intraparticle water. The situation described here is analogous to that present in organic cation exchangers where the water contained in the swelled resin beads contains signficant amounts of cation and/or hydronium ions. Any amount of cations in solution, even trace amounts, would exchange with the intraparticle hydronium ion to produce a measurable acidity in the external solution. Tin oxide should then be able to exchange cations in acid solution and reference to Figure 1 shows that this is true. In contrast to tin oxide, hydrous zirconia has a more highly protonated surface and yields basic solutions by donation of protons from the interparticle water to the surface, and this is reflected in its ion exchange behavior also (Figure 1). It is well to point out here that precipitation of hydrous zirconia in acid solutions allows an appreciable amount of anion to be incorporated into the gel. Washing with base or refluxing results in displacement of the anions by hydroxyl groups while refluxing also results in particle growth.[35]

2. Conductivity Behavior of Particle Hydrates

The foregoing picture of hydrous oxides would indicate that they should exhibit an appreciable proton conductivity. Conductivities have been measured for both tin and zirconium hydrous oxides of known water content by the complex admittance method.[33] The results are shown as a function of temperature in Figure 3. Two mechanisms of proton motion in aqueous media have been described,[41] a drift of hydrated protons in the solution and a Grotthus mechanism. In particle hydrates with high water content the latter mechanism would be expected to dominate. Increasing the acidity or basicity and water content, as well as the surface areas, would be expected to increase the conductivity. Although conductivities for several additional hydrous oxides have recently been determined,[42] a quantitative correlation with theory has not yet been achieved. A further discussion of the conductivity mechanism is given in section II.B.3.

3. Catalytic Applications

Hydrous oxides such as those of zirconium and titanium are utilized as catalysts or catalyst supports.[43,44]

For many such uses high surface areas are required. It is clear from the foregoing description of the oxides that high surface areas require small particle size. A cubic particle 25 Å on a side would have a surface area of about 600 m^2/g. Thus, by rapid precipitation in the cold with good stirring, one can prepare particles o f this size. To ensure the absence of impurities, the oxides need to be washed with ammonia in order to remove any exchanged ions, dried under vacuum, and calcined at low temperature. Heating to temperatures much above 400 °C results in agglomeration of particles with loss of surface area. An excellent exposition of these processes for hydrous zirconia has been given by Rijnten.[45]

B. Framework Hydrates

We shall illustrate the nature of these oxides by describing two of them, antimonic acid or antimony pentoxide and manganese dioxide.

1. Antimony Oxides

Hydrous antimony oxide, $Sb_2O_5 \cdot xH_2O$, can be prepared in amorphous and crystalline forms. The amorphous product is unstable, crystallizing on aging or on treatment with acid at elevated temperatures.[46] It is now well established that three crystalline phases exist: a pyrochlore phase, a layered phase with an ilmenite-like structure, and a cubic phase.[47] The most common form of hydrous antimony oxide was referred to in the early literature as polyantimonic acid because of its high proton content (ion exchange capacity of 5.1 mequiv/g).[48,49] Powder pattern X-ray diffraction data were analyzed to show that this compound actually had a pyrochlore structure[33] and a composition represented by the formula $(H_3O)_2Sb_2O_6 \cdot H_2O$. This formula yields a theoretical ion exchange capacity of 5.08 mequiv/g[33] and fits the thermogravimetric curve closely.[49] Although the hydronium ions and water molecules were not located, they are thought to reside in the cavities with the oxygen atoms centered on the 16d and 8b positions of the ideal cubic space group.[50] The rigid pyrochlore framework imposes size limitations on cation selectivity. Abe[51] observed the following selectivity order: $Na+ > K^+ > Rb^+ > Cs^+ > Li^+$. In order for these hydrated ions to exchange into the pyrochlore cavities, they need to be partially dehydrated. The selectivity order represents a compromise between cation size and hydration energy. For lithium ion the hydration energy term must dominate, preventing high uptake.

The ilmenite-type (layered) antimony oxide was prepared by acid treatment of $KSbO_3$, which itself has an ilmenite structure.[47] In the potassium compound the structure is a true three-dimensional one, but upon replacement of the K^+ ions with hydrogen (hydronium) ions, the structure is broken down into layers with the exchangeable hydrogen ions situated beteen the layers. However, the composition is very similar to that of the pyrochlore compound.

Antimonic acid with a cubic structure was prepared by acid treatment of cubic $KSbO_3$. The latter compound was in turn synthesized by heating $K_2H_2Sb_2O_7 \cdot 4H_2O$ in a sealed gold tube at 500–700 °C under 3-kbar pressure for 10 h. Its formula is $(H_3O)^+HSb_2O_6$ or $HSbO_3 \cdot xH_2O$. NMR spectra for all three polymorphs

TABLE 2. Summary of Conductivity and NMR Data for
$HMO_3 \cdot xH_2O$ Compounds at High Humidity[a]

M	structure	$\sigma(30 \, ^\circ C)$, $\Omega^{-1} \, cm^{-1}$	$E_a(\sigma)$, kcal/mol	$E_a(NMR)$, kcal/mol
Sb	cubic $KSbO_3$ type	8.7×10^{-4}	9.1 ± 0.1	2.3 ± 0.4
Sb	layer	2.2×10^{-3}	4.3 ± 0.1	2.3 ± 0.4
Sb	pyrochlore	3.2×10^{-3}	4.6 ± 0.1	2.3 ± 0.4
Nb	pyrochlore	1.5×10^{-4}	5.0 ± 0.5	5.3 ± 0.8
Ta	pyrochlore	1.4×10^{-4}	6.0 ± 0.1	6.0 ± 0.8

[a] From ref 47, with permission.

exhibit a three-peak pattern indicative of hydronium ion.[47] This does not preclude the presence of free protons, so the choice between the two formulas for the cubic polymorph is still not clear.

2. Niobium and Tantalum Oxides

Hydrous niobium and tantalum oxides, as prepared by hydrolysis of the pentahalides or addition of base to aqueous acid solutions, are amorphous and behave as though they are particle hydrates.[52] However, their cation exchange capacities, 3.3 mequiv/g for niobium oxide and 2 mequiv/g for tantalum oxide, are exceptionally high for particle hydrates. Cations are exchanged under fairly acid conditions, indicating a high level of hydronium ions in the interparticle water. This type of behavior would be expected of M(V) hydrates because the high charge on the metal results in strong bonds to oxygen and strong repulsion of the proton. Anions are also taken up in highly acid solution by these hydrates but they can be eluted with NH_3.

A pyrochlore form of niobium and tantalum oxides can also be prepared by treating the thallium(I) niobate or tantalate with acid.[47,53,54] The general formula is $(H_3O^+)HM(V)_2O_6$. NMR spectra indicate the presence of both hydronium ions and free protons in accord with this formula.[47]

A related reaction to the one described above involved the preparation of $HNbO_3$ and $HTaO_3$ by acid treatment of the corresponding lithium compounds at 95–100 °C.[55] The transformation is a topotactic one involving a transition from the rhombohedral lithium niobate structure to a cubic perovskite one. $LiNbO_3$ and $LiTaO_3$ are ferroelectric and nonlinear optical materials of considerable industrial and theoretical importance. Since crystals of these compounds are often cleaned in boiling acid, it is likely that surface exchange will take place. Subsequent heating of the crystal will remove the protons as water, leaving a lithium-deficient surface layer of composition $M_2O_5(Li_2O)_{1-x}$. Partially exchanged $LiNbO_3$ is of particular interest since the proton exchange produces a large change in index of refraction of the crystals.[56] Therefore, a more detailed study of the structural changes in the system $Li_{1-x}H_xNbO_3$ was undertaken.[57,58] A number of distinct phases were discovered in this system along with several phase transitions. An order–disorder mechanism was invoked to account for these observations.

3. Proton Conductivity of Hydrous Oxides

Proton conductivity data for the framework hydrates are summarized in Figure 4 and Table 2.[47] The conductivity of the protonated species is at least 2 orders of magnitude higher than that of the corresponding cation species. This effect has been attributed to dif-
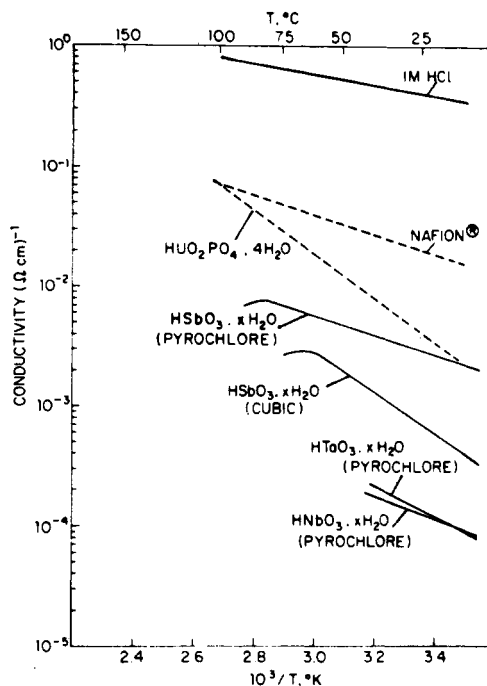

Figure 4. Proton conductivities for $HMO_3 \cdot nH_2O$ (M = Sb, Nb, Ta) compared to other good proton conductors. Values for 1 M HCl are also shown for comparison. (From ref 47, with permission.)

ferent mechanisms of conduction of the two species.[47] The high conductivities of the protonated framework hydrates are thought to result from a Grotthus mechanism.[41,60] In this conduction process hydronium ions must reorient to the proper position for proton transfer to occur. Reference to Table 2 shows that for the antimony framework hydrates the activation energy as measured by NMR is lower than that obtained from the slope of the conductivity curves. According to Chowdhry et al.,[47] the NMR process measures hydronium ion reorientation while the conduction process measures proton hopping as well as the reorientation. The high activation energy observed for the protonated cubic polymorph is the same as that for K^+ ion conduction in $KSbO_3$ (see Figure 8, ref 47). In the potassium compound conduction must involve translation of the ions. Therefore, in the cubic protonated hydrate the conduction process likely involves translation also (eq 4). In the case of the niobium and tantalum hydrates,

$$E_a(\sigma) = E_a(NMR) + E_a(hopping) + E_a(transl) \quad (4)$$

half the protons must be bonded to lattice oxygens. The conduction process may involve hopping of protons from hydronium ion to the lattice, in turn facilitating lattice-to-water hopping. In such a process both the NMR- and conduction-determined E_a values are the same and therefore must be controlled by the hopping mechanism.

Chowdhry et al. point out[47] that the NMR E_a values for the pyrochlore hydrates scale inversely as the electronegativity values of the metal atoms. The M–O bond is more covalent in the Sb compound than in Nb and Ta since it has the higher electronegativity. Hence the Brøsted acidity of the Sb compounds should be higher and the proton more delocalized, accounting for its lower E_a value. Particle hydrates also conduct by a Grotthus mechanism when sufficient water is present in the pores.[33]

TABLE 3. Data for Mn(IV) Oxides with Tunnel Structures

mineral name	approx formula	structural features	unit cell dimensions
pyrolusite	β-MnO_2	octahedra forming 1 × 1 tunnels	a = 4.39 Å, c = 2.87 Å (tetragonal)
ramsdellite	MnO_2	octahedra forming 2 × 1 tunnels	a = 4.39 Å, b = 9.27 Å, c = 2.87 Å (orthorhombic)
nsutite	γ-MnO_2 or γ-MnO_x	intergrowths of pyrolusite and ramsdellite	a = 9.65 Å, c = 4.43 Å
hollandite (α-MnO_2)	$BaMn_8O_{16}\cdot xH_2O$ (ideal)	2 × 2 tunnels, lower valent Mn present	a = 9.96 Å, c = 2.86 Å
cryptomelane	$KMn_8O_{16}\cdot xH_2O$	members of hollandite family	a = 9.84 Å, c = 2.86 Å
coronadite	$PbMn_8O_{16}\cdot xH_2O$		
manjiroite	$NaMn_8O_{16}\cdot xH_2O$		
psilomelane	$Ba_2Mn_5O_{10}\cdot xH_2O$	3 × 2 tunnels parallel to b axis	a = 9.56 Å, b = 2.88 Å, c = 13.85 Å, β = 92.5°
(romanechite)	(K^+ substitution for Ba^{2+})		
todorokite	$(Na,Ca,Mn)Mn_3O_7\cdot xH_2O$	3 × 3 tunnels, monoclinic cell	a = 9.75 Å, b = 2.85 Å, c = 9.59 Å, $\beta \simeq$ 90°
ϵ-MnO_2	$MnO_{1.9}$–$MnO_{1.98}$ or ideally Mn_4O_8OH	like γ-MnO_2, fibrous form	a = 4.85 Å, b = 8.90 Å, c = 2.80 Å (c = 2.80 × 3 = 8.40 Å in the supercell)

NMR studies of two particle hydrates, $SnO_2\cdot nH_2O$ and $TiO_2\cdot nH_2O$, have been carried out in order to gain further insight into the conductivity mechanism of this class of compounds.[61] Three types of protons were recognized: those associated with hydroxyl groups, water, and hydronium ions. Two sets of spin relaxation constants and correlation times were observed. Thus, the particle hydrate model (section II.A) was extended to include protons present in micropores of less than 100 Å (region B) and those present in macropores of larger diameter (>1000 Å). Surface hydroxyl groups are associated with both types of pores, which allows exchange of protons between the different pores to occur. The pores are formed by the joining of oxide particles to form agglomerates containing cracks and fissures. The solution in the macropores is thought to be almost liquid-like, while that in the micropores will be more constrained and thus exhibit a longer correlation time. Hydrous tin oxide exhibits two activation energies in its conductivity behavior (Figure 3), with values of 9.3 kcal/mol below 288 °C and 5.6 kcal/mol above this temperature. At the lower temperature the conductivity measures the activation energy for motion of protons in the macropores. At higher temperature, motion through the micropores becomes rate determining. Hydrous titania (and zirconia) exhibits a single activation energy of 6.9 kcal/mol, indicating transport in the macropores over the entire temperature range. As water is lost, other transport mechanisms must become operative.

4. Hydrous Oxides with Tunnel Structure: MnO_2

The cation exchange behavior of manganese dioxide is important in connection with measurements of the potentials in electrochemical cells and batteries. Electrical potential depends upon the pH of the surrounding solution, which in turn is influenced by the release or uptake of protons by the MnO_2 electrode. The cation exchange properties of manganese dioxide were first reported by Ghosh[62] and later expanded upon by Kozawa.[63] Initially it was thought that the ion exchange reaction took place only on the surface and on this basis Brenet et al.[64,65] formulated manganese dioxides, precipitated from aqueous systems, as oxo hydroxides, eq 5. In this formula n is the degree of ox-

$$MnO_{n-z}(OH)_{2z}\cdot mH_2O \qquad (5)$$

idation (close to 2) and z is a small fraction. Later work has shown that macroamounts of ions could be exchanged.[66,67] Tsuji and Abe[67] prepared their exchanger
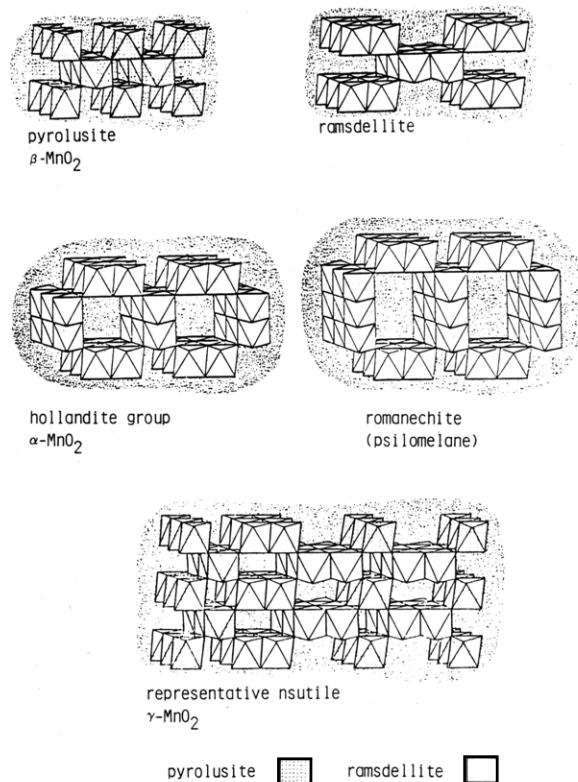

Figure 5. Various forms of MnO_2 with tunnel structures. (From: Burns, R. G.; Burns, M. B. *Manganese Dioxide Symposium*, Tokyo, 1981; Vol 2, Chapter 6).

by addition of Mn(II) to a $KMnO_4$ solution. X-ray diffraction patterns showed that the product had a cryptomelane structure in which hydronium ions were presumably located in the tunnels.

Figure 5 depicts schematically the various forms of MnO_2. A more complete listing is given in Table 3. It should be noted that hollandites and other members of the hollandite family are not true manganese dioxides but contain mono- or divalent cations in the tunnels. On treatment with acids, the cations are exchanged for hydronium ions. Thus, theoretically a completely new family of ion exchangers is possible. The exchanger described by the Russian workers[66] was prepared electrolytically from $MnSO_4$. This exchanger exhibited ion exchange capacities of the order of 4 mequiv/g. Shen and Clearfield[68] also used an electrolytic method to prepare hydrated manganese dioxides. They found that the exchange capacity was a maximum for the products prepared at temperatures of less than 25 °C and de-

creased with increasing temperature of preparation. The manganese dioxide prepared at 95 °C exhibited only surface exchange. For preparations obtained below 25 °C the ideal formula is $(MnO_{1.75})_2OH \cdot xH_2O$. All of the protons could be exchanged by Li^+, but lesser amounts were exchanged as the exchanging cation size was increased. The exchanger is thought to have a γ-MnO_2-like structure (Figure 5), but its amorphous nature sufficiently disorders the tunnels to allow some large ions to be exchanged.

When the Li^+-exchanged form of the γ-MnO_2 was heated to 500 °C, it was converted to the spinel $LiMn_2O_4$.[68] The reaction could be formulated as

$$(MnO_{1.75})_2OLi \rightarrow LiMn_2O_4 + {}^1/_4O_2 \qquad (6)$$

Treatment of the spinel with dilute acid converted it to HMn_2O_4 with retention of the spinel structure. The higher the temperature to which the lithium-exchanged manganese dioxide was heated, the less Li^+ was released on acid treatment. In the spinel form, HMn_2O_4, the exchanger is highly specific for Li^+.

The sodium ion exchanged phase of the electrolytically prepared hydrous MnO_2 formed an as yet unidentified phase on heating to 500 °C. However, in contact with boiling water this phase was converted to birnessite with uptake of water. Birnessite is a layered form of MnO_2, usually termed δ-MnO_2, which contains sodium ions.[69,70] The formula proposed by Shen and Clearfield,[68] $Na_4Mn_{14}O_{27} \cdot 9H_2O$, and that of the protonated form obtained by them from the sodium phase, $H_4Mn_9O_{18} \cdot 7H_2O$, differ from the corresponding formulas given earlier by Giovanoli.[69,70] Many sodium, potassium, or other cation phases of manganese are known, some with tunnel structure and others with layered structure,[69-75] some of which exhibit ion exchange behavior.[67,76-79] It may thus be possible to prepare proton forms of many of these compounds and exchange different ions into them. Subsequent heat treatment may then produce new as yet undiscovered phases. The same may be true in the case of other framework-type hydrous oxides.

III. Ion Exchange in Mixed Oxides

The ease of ion exchange in classes of compounds such as zeolites, hydrous oxides, and acid phosphates (section IV) may be understood in terms of the presence of interconnected cages, channels, or layers of sufficient dimensions to allow ion transport. Fast ion conductors such as β-alumina (section V.B) and NASICON (section V.A) also undergo ion exchange as well as fast ion transport. They have rigid frameworks but the mobile cations occupy only a part of the sites allowing transport into empty sites. A preliminary consideration of thermodynamic and kinetic factors led England et al.[37] to conclude that ion exchange may be a widespread phenomenon in inorganic solids, well below their sintering temperatures, and that high concentrations of vacancies may not be necessary. These points will be discussed in what follows.

A. Ternary Oxides

1. ABO₂-Type Structures

In β-$NaAlO_2$ the Na^+ and Al^{3+} ions occupy alternate tetrahedral sites in a hexagonal close-packed wurtzite

TABLE 4. Ion Exchange Reactions of Layered α-$NaCrO_2$-Type Structures[a]

substrate	structure	reagent	product	structure
α-$LiMO_2$ (M = Co, Cr, Rh)	α-$NaCrO_2$	$Pd + PdCl_2$	$PdMO_2$	delafossite
α-$LiFeO_2$	α-$NaCrO_2$	$CuCl(l)$	$CuFeO_2$	delafossite
α-$LiMO_2$ (M = Co, Cr, Rh)	α-$NaCrO_2$	$AgNO_3(l)$	$AgMO_2$	delafossite

[a] From ref 37, with permission.

structure.[80] Geissner et al.[81,82] treated β-$NaAlO_2$ in melts containing Ag^+, Cu^+, and Tl^+ and were able to totally replace the Na^+ by utilizing a large excess of cations in the melt. Similar reactions were obtained with aluminates which possess a cristobalite structure.

In the α-$NaCrO_2$ structure both the Cr^{3+} and Na^+ are octahedrally coordinated in alternate layers. Lithium ion exchange was carried out in excess molten $LiNO_3$ for 24 h at 300 °C. Close to 100% of the Na^+ was exchanged with a corresponding formation of $LiCrO_2$.[37] Aqueous exchange of H^+ for Na^+ was also carried out at room temperature with a 25% HNO_3 solution. A 92% exchange was observed with formation of $HCrO_2 \cdot 0.92H_2O$. Heating to 400 °C yielded $HCrO_2$. Table 4 summarizes work by Shannon et al.[83] in which they converted lithium salts of several metals with the α-$NaCrO_2$ structure to delafossite-type phases.

2. Spinels

Joubert and Durif[84,85] have reported an ion exchange reaction for the spinel $(Li_{1.5}Zn_{1.5})_{tet}(Ge_{4.5}Li_{1.5})_{oct}O_{12}$ to produce $(Zn_3)_{tet}(Ge_{4.5}\square_{1.5})_{oct}O_{12}$. The reaction was carried out in molten $ZnSO_4$ at 500 °C for 3 weeks. A similar exchange reaction was carried out[80] on $Li_4Ti_5O_{14}$, in which the ion arrangement is $(Li_3)_{tet}(LiTi_5)_{oct}O_{12}$. A total of 68% of the Li^+ was replaced by Zn^{2+} in 4 days at 500 °C. In all the spinel reactions, vacancies are created only in the octaheral holes. Exchange does not proceed to the point where tetrahedral vacancies are created.

We have already discussed the case of $LiMn_2O_4$ in section II.B.4. The ready exchange for H^+ occurs because of incomplete crystallization of the compound at 500 °C which provides defects that facilitate exchange. It should be mentioned that Hunter[86] claimed to have removed all the Li^+ from $LiMn_2O_4$ by acid treatment to yield λ-MnO_2. He explained this transformation on the basis of a surface reaction to remove Li^+ followed by a disproportionation of Mn^{3+} to form soluble Mn(II) and insoluble Mn(IV). A possible explanation for the difference in behavior reported by Hunter and the simple ion exchange reaction[68] lies in his use of strong acid solutions whereas the exchange reaction was carried out in 0.1 M acid. Another case in point is that of Fe_3O_4 or magnetite. It has an inverse spinel structure $(Fe^{III})_{tet}(Fe^{II}Fe^{III})_{oct}O_4$. Natural magnetite has been used to remove radioactive cations from nuclear waste streams.[87] More recently, magnetite was prepared in situ and found to remove 5–50 times as many ions as did ferric hydroxide.[88] Presumably the sequestered ions replace iron ions in both the tetrahedral and octahedral holes but no evidence for this was presented. However, it might be expected from what has been already described in this report that poorly crystallized spinels may readily exchange ions with aqueous electrolytes
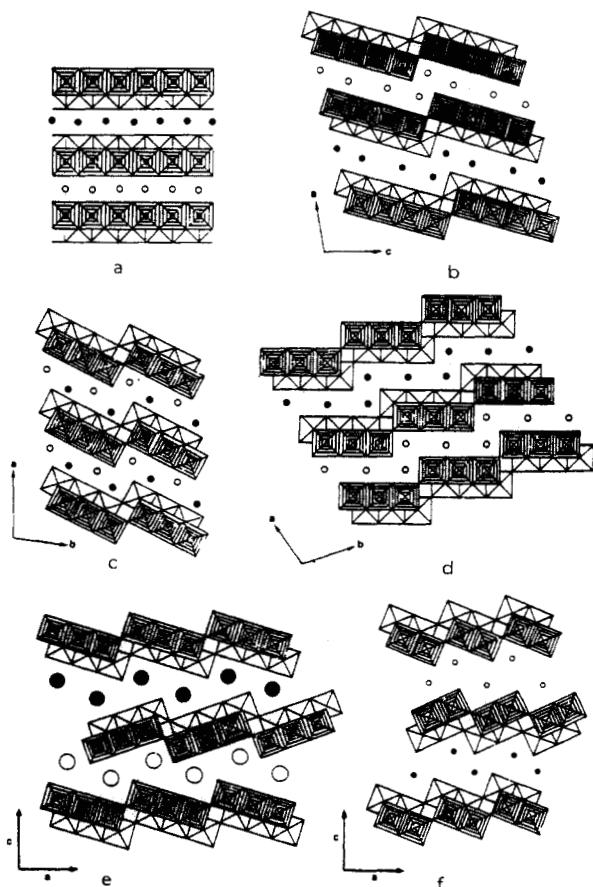
Figure 6. Idealized structure of titanates and titaniobates with a layer structure: (a) $A_xTi_{2-x}M_xO_4$; (b) $Tl_2Ti_4O_9$; (c) $Na_2Ti_3O_7$; (d) $K_3Ti_5NbO_{14}$; (e) $CsTi_2NbO_7$; (f) $KTiNbO_5$. (From ref 114, with permission.)

and well-crystallized spinels would behave similarly with molten salts. Such reactions may prove useful in doping ferrites.

3. Metal Titanates

Alkali metal titanates have been synthesized which conform to either of the following two series: $M_2Ti_nO_{2n+1}$ and $Na_4Ti_nO_{2n+2}$. In the former series, members with $n = 1$–9 have been prepared[89-97] and in the latter series, compounds with n odd ($n = 1, 3, 5$).[96-100] $K_2Ti_2O_5$, $Na_2Ti_3O_7$, $Na_2Ti_4O_9$, and $Na_4Ti_5O_{12}$ have layered structures of the type shown in Figure 6b,c.[101] On the other hand, $Na_2Ti_6O_{13}$ and $K_2Ti_6O_{13}$ have a rigid structure in which three octahedra share edges and are joined through corners to similar chains of three octahedra to form tunnels (Figure 7).[94] Ion exchange behavior has been demonstrated in $K_2Ti_2O_5$, $Na_2Ti_3O_7$, and $M_2Ti_4O_9$. In fact alkaline earth tetra-titanates can be prepared from $TlTi_4O_9$ by ion exchange.[92]

Treatment of the tri- and tetratitanates with HCl converted them to $H_2Ti_3O_7$ and $(H_3O^+)HTi_4O_9$, respectively.[101] Dehydration of the latter compound yielded $H_2Ti_8O_{17}$, which was assigned a tunnel structure.[101] Further dehydration resulted in the formation of $TiO_2(B)$, a new form of titanium dioxide.[97,101] It would be interesting to determine whether additional novel oxides would result from partial and complete dehydration of protonated oxides under mild conditions. Reversibility of exchange was found to be difficult as even the use of 1 M base only partially ex-
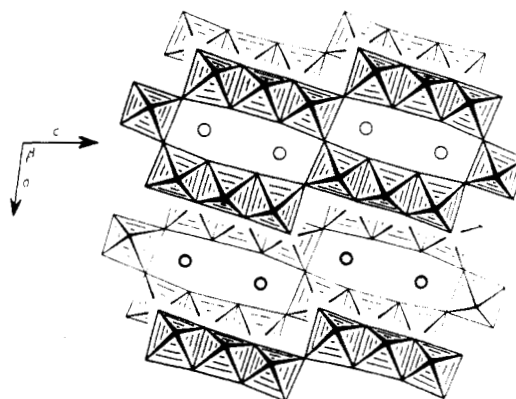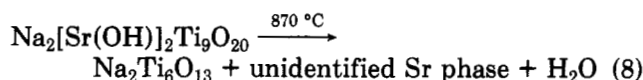

Figure 7. $Na_2Ti_6O_{13}$ in projection. The corners join adjacent sheets to form a framework enclosing tunnels. Two sodium ions (circles) are present in a unit tunnel which contains three pseudocubic positions. (From ref 94, with permission.)

changed out the protons. Apparently the shrinkage of the cell volume on protonation makes reversibility of exchange difficult. However, subsequent work produced half, three-quarter, and fully exchanged Na^+ and K^+ phases from the acid forms.[103-105] A one-quarter exchanged phase was also obtained in the K^+ system. Structural explanations for these exchange data have been presented. The tri- and tetratitanates in the acid form were also found to form amine intercalates by ion exchange of alkylammonium salts for H^+.[106] Only modest conductivities were exhibited by the tri- and tetratitanates, but a marked improvement was observed when a small amount of Nb^{5+} isomorphously replaced Ti^{4+}. This increase was attributed to a slight expansion of the lattice.[107]

A new sodium titanate[108] was prepared by the action of NaOH on anatase. It has been shown to approximate the formula $Na_4Ti_9O_{20}\cdot nH_2O$[109] but to differ from $Cs_4Ti_4O_{20}$[110] and $Ba_4Ti_9O_{20}$. The latter compound is reported to have a hollandite structure[111] whereas the hydrated sodium nonatitanate has a layered structure.[109] Complete exchange of H^+ for Na^+ is readily accomplished. The nonatitanate shows promise as an exchanger for the removal of $^{90}Sr^{2+}$ from nuclear waste streams.[112] Uptake of Sr^{2+} by $Na_4Ti_9O_{20}$ yielded $Na_2(SrOH)_2Ti_9O_{20}$ because of the high pH produced by hydrolysis of the sodium phase whereas $H_4Ti_9O_{20}$ was converted to $Sr_2Ti_9O_{20}$.[113] Heating these exchanged products resulted in the following reactions:

$$Sr_2Ti_9O_{20} \xrightarrow{600\ 8°C} 2SrTiO_3 + 7TiO_2 \qquad (7)$$

$$Na_2[Sr(OH)]_2Ti_9O_{20} \xrightarrow{870\ °C}$$
$$Na_2Ti_6O_{13} + \text{unidentified Sr phase} + H_2O \quad (8)$$

B. Quaternary Oxides

1. Mixed-Metal Titanates

Several mixed niobium and tantalum titanates have been synthesized and shown to possess ion exchange properties. These include $ATiNbO_5$,[115,116] $CsTi_2NbO_7$,[117] $A_3^+Ti_5NbO_{14}$,[118] KTi_3NbO_9,[119] and a nonstoichiometric series $K_{1-x}Ti_{1-x}Nb_{1+x}O_5$,[115,116] related to the first listed compound. The structures of these compounds are layered ones built of octahedra sharing edges and forming a double plane as shown in Figure 6a. The
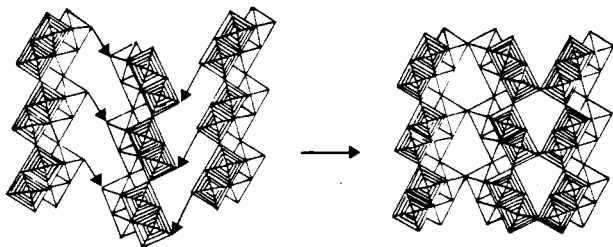
Figure 8. Topotactic formation of the empty tunnel structure $Ti_2Nb_2O_9$ by condensation of two $[TiNbO_5]^-$ layers from the layer oxide $HTiNbO_9$. (From ref 114, with permission.)

other structures are derived from this one by shearing the layers in the direction perpendicular to its plane, every third octahedron for $CsTi_2NbO_7$ and $K_3Ti_5NbO_{14}$ and every second octahedron for $K_{1-x}Ti_{1-x}Nb_{1+x}O_5$.[114] In some cases the layers are parallel but in others, such as $ATiNbO_5$, the layers are related by a glide plane.[117] In each case the A^+ ions lie between the planes and serve to bind them together by electrostatic attractions.

Protonated forms of the titanoniobates can be prepared by treatment of their alkali metal forms with acid. $ATiNbO_5$ oxides are easily exchanged, yielding the unhydrated protonic oxide $HTiNbO_5$.[114,115] In contrast, $CsTi_2NbO_7$ requires treatment with concentrated acid and forms a hydrate, $HTi_2NbO_7 \cdot 2H_2O$. It dehydrates at 100 °C. $A_3Ti_5NbO_{14}$ compounds are much less reactive and cannot be completely exchanged by acids. The highest protonic content produced by direct reaction is $K_{0.5}H_{2.5}Ti_5NbO_{14}$. However, by exchanging Na^+ for K^+ in this compound one obtains $H_{1.5}Na_{1.5}Ti_5NbO_{14}$ and $HNa_2Ti_5NbO_{14}$, which in acid solutions are converted to $H_3Ti_5NbO_{14} \cdot H_2O$. Removal of the water destroys the compound.

An interesting product can be prepared by splitting out water from $HTiNbO_5$. The anhydrous compound $Ti_2Nb_2O_9$ is formed because the layers come together in the manner shown in Figure 8. The resultant mixed oxide contains tunnels and because of its open structure can intercalate lithium and sodium to form $A_xTi_2Nb_2O_9$-type compounds.[114]

Because of their acidic character, the protonic oxides readily intercalate amines, and an extensive literature has developed on this subject.[114,120–122] Lal and Howe[123] have measured the conductivity of protons in $HTi_2NbO_7 \cdot 2H_2O$. The water molecules in this compound form a double layer between the oxide sheets, which were expected to facilitate proton transport. Conductivities (17–21 °C) were $(2 \pm 1) \times 10^{-4}$ Ω^{-1} cm^{-1} as pressed pastes and $(9 \pm 3) \times 10^{-5}$ to $(8 \pm 4) \times 10^{-6}$ Ω^{-1} cm^{-1} as pressed powders.

A series of compounds has been prepared over the years by isomorphous replacement of Ti^{4+} in TiO_2 by M^{2+} and M^{3+} cations. The general composition of these compounds is $A_{2x}Ti_{2-x}M^{II}_xO_4$ (M(II) = Mg, Zn, Ni, and Cu and A is an alkali metal) and $A_xTi_{2-x}M^{III}_xO_4$ [M(III) = Fe(III), Mn(III)].[124] The structures consist of both TiO_6 and MO_6 octahedra arranged in two different ways. When $2x$ is less than 0.5 the structure is of the hollandite type with the A^+ (K^+, Rb^+, Tl^+, Cs^+) ions in the tunnels.[125–128] At higher values of $2x$ (0.6–0.8) the compounds have a layered structure in which the Ti–Mg octahedra share edges and corners in a corrugated fashion.[129] England et al.[130] determined the ion exchange behavior of one of the latter type compounds
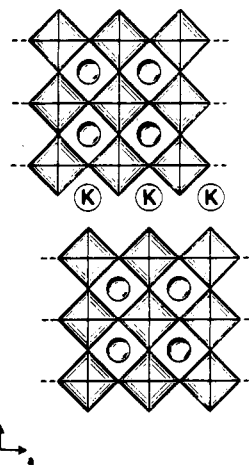

Figure 9. Schematic representation of the structure of $KCa_2Nb_3O_{10}$. The shaded squares represent NbO_6 octahedra in projection, and the circles within the layers are the calcium atoms. The c axis is perpendicular to the layers. (From ref 135, with permission.)

with composition $Cs_{0.7}Ti_{1.65}Mg_{0.35}O_4$. Since there are $1-2x$, or in this case, 0.3 mol of vacant Cs^+ sites, ion exchange should be facilitated. Li^+, Na^+, and K^+ could be exchanged for Cs^+ from fused-salt reactions in the 300–400 °C temperature range in 12 h. Aqueous exchange required up to 4 days for complete reaction. Concentrated or even strong acid solutions dissolve the titanate, but the protonated form could be obtained by use of dilute acid solutions.

2. Complex Niobates and Tantalates with Tunnel or Perovskite Structures

Recently, Dion et al.[131] synthesized a new family of layered oxides with the general formula $ACa_2Nb_3O_{10}$ (A = K, Rb, Cs, Tl).[131–133] The layers consist of perovskite slabs separated by A^+ ions (Figure 9). Because such compounds have a lower layer charge density than strontium titanates of the type $Sr_2[Sr_{n-1}Ti_nO_{3n+1}]$,[134] ion exchange was observed to occur under relatively mild conditions whereas the strontium titanates did not react under similar conditions. Following this discovery, Jacobson et al.[135] were able to prepare a series of such layered perovskites with the general formula $K[Ca_2Na_{n-3}Nb_nO_{3n+1}]$ ($3 \le n \le 7$). The layer thickness was found to increase by about 3.9 Å for each increase in n, reaching a value of 27 Å for $n = 7$. Protonic and hydronium ion phases of each series member could be prepared by exchange of the K^+ ion phases in 6 M HCl at 60 °C for 16 h.[135,136] Alkylamines could then be intercalated into the solid acids, forming interesting bilayer structures.[135,137]

Members of the layered perovskite family with $n = 2$ were prepared[138] by substituting La^{3+} for Ca^{2+}. The resultant compounds, $ALaNb_2O_7$ (A = Li, Na, K, Rb, Cs, NH_4), consist of double perovskite slabs with A^+ ion layers between them. The solid acid $HLaNb_2O_7$ was obtained by acid treatment followed by dehydration. It exhibited Brønsted-type acidity and intercalated amines.

Two interesting series of niobates with proposed formulas of $A_{12}M^V_{30}M'^{VI}_3O_{90}$ and $A_{10}M_{29.2}O_{78}$ have been synthesized.[139,140] The former series has members with M(V) = Nb and Ta and M(VI) = W and Mo while the latter contains M(V) as either Nb or Ta. The structure
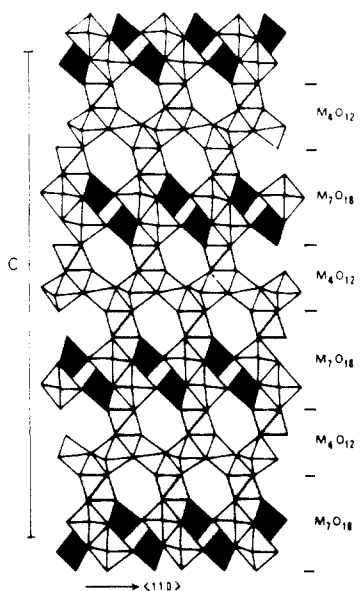
Figure 10. Schematic representation of the stacking of groups in $A_{12}M_{33}O_{90}$. (From ref 139, with permission.)
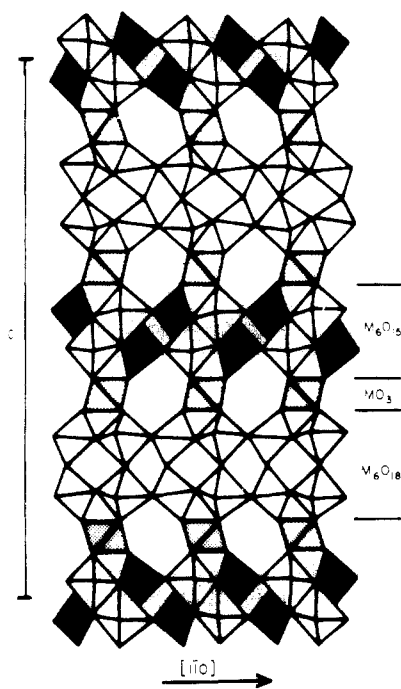

Figure 11. Representation of the stacking along the c axis of the hexagonal cell of the compound $A_{10}M_{29.2}O_{78}$. (From ref 140, with permission.)

of the $A_{12}M_{33}O_{90}$-type compounds is built up of M_7O_{18} pyrochlore-like units[141] interleaved with M_4O_{12} units (Figure 10).[139,142] Similarly, the $A_{10}M_{29.2}O_{78}$ compounds are built up of intergrowths of M_6O_{18}–MO_3–M_6O_{15} units as shown in Figure 11.[140] Phases which could not be prepared by the direct reaction of oxide mixtures, such as the hydronium and silver ion phases, were obtained by ion exchange. An interesting solid–solid exchange reaction in which K^+ replaced Tl^+ according to eq 9 was

$$Tl_{12}M_{30}M'_3O_{90} + KCl \rightarrow K_{12}M_{30}M'_3O_{90} + TlCl\uparrow \quad (9)$$

possible due to the volatility of TlCl. This reaction is similar to those carried out by Clearfield et al. with zirconium phosphate[143] and H-zeolites.[144] These latter reactions depended upon the volatility of HCl.

TABLE 5. Some Important Acid Salts of Tetravalent Metals with Layered Structure of the α-Type

compd	formula	inter-layer dist, Å	ion exchange capacity mequiv/g
titanium phosphate	$Ti(HPO_4)_2\cdot H_2O$	7.56	7.76
zirconium phosphate	$Zr(HPO_4)_2\cdot H_2O$	7.56	6.64
hafnium phosphate	$Hf(HPO_4)_2\cdot H_2O$	7.56	4.17
germanium(IV) phosphate	$Ge(HPO_4)_2\cdot H_2O$	7.6	7.08
tin(IV) phosphate	$Sn(HPO_4)_2\cdot H_2O$	7.76	6.08
lead(IV) phosphate	$Pb(HPO_4)_2\cdot H_2O$	7.8	4.79
titanium arsenate	$Ti(HAsO_4)_2\cdot H_2O$	7.77	5.78
zirconium arsenate	$Zr(HAsO_4)_2\cdot H_2O$	7.78	5.14
tin(IV) arsenate	$Sn(HAsO_4)_2\cdot H_2O$	7.8	4.80

C. Conclusions

In the foregoing section we have seen that ion exchange can occur in a wide variety of oxide structure types, including framework or tunnel structures, layered compounds, and even lattice structures with close-packed oxygens. That facile ion exchange may occur in structures which are easily expandable (layered structure or hydrate) and those with tunnels or gross nonstoichiometry is easy to comprehend. To the very large number of such compounds described above must be added those that will be described below such as the group IV (groups 4 and 14) and related phosphates, β-alumina, and silicophosphates. It is then clear that there is an abundance of inorganic compounds which meet the requirements for facile ion exchange. However, the reader should also keep in mind that many compounds not normally considered to be ion exchangers, such as the spinels and the ABO_2 class of compounds, may be induced to exchange under forcing conditions.

IV. Group IV (Groups 4 and 14) Phosphates and Related Compounds

A. α-Type M(IV) Layered Phosphates

1. Structure and Ion Exchange Behavior

This group of compounds consists of phosphates, arsenates, and mixed phosphate–arsenates of both group IVA (group 14) and group IVB (group 4) elements. A partial list of the α-type compounds is given in Table 5. A number of comprehensive reviews on various aspects of the properties and behavior of these compounds have been published recently,[1,2,148] including materials aspects,[145] ion exchange,[146] catalysis,[147] and membranes.[149] Therefore, we shall confine ourselves to those aspects of this subject which have relevance to solid-state chemistry and to newly synthesized compounds and their properties. By way of introduction we remind our readers that members of this class of compounds are obtained as amorphous gels when prepared by rapid precipitation in the cold, but refluxing in solubilizing media slowly transforms them into crystals.[23,39] The slow transformation, in the case of zirconium phosphate, allows the operator to build in the level of crystallinity desired for a particular purpose. The crystals have a layered structure in which the metal atoms lie nearly in a plane and are bridged by phosphate groups as shown in Figure 12. Thus three phosphate oxygens bond to metal atoms so that the remaining phosphate oxygen, which is bonded to a proton, points into the interlayer space. The layers are
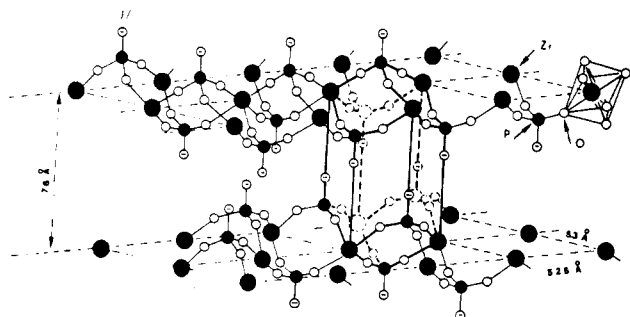
Figure 12. Idealized structure of α-zirconium phosphate showing one of the zeolite cavities created by the arrangement of the layers. (From Alberti, G. In *Study Week on Membranes*; Passino, R., Ed.; Pontificiae Academie Scientarum Scripta Varia: Rome, 1976; p 269 (with permission)).
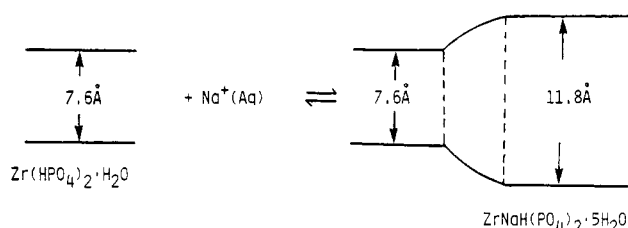

Figure 13. Schematic representation of layer expansion by ion exchange according to Alberti.[148] Region between dashed lines is solid solution region. (After ref 148, with permission.)

staggered, forming a network resembling a hexagonally shaped cavity (heavy outline in Figure 12) with the water molecule in the center.

In this α-layer the metal atoms are six-coordinate and the phosphates tetrahedral, forming T–O–T-type layers as in smectite clays. The major difference is that the phosphate groups are in inverted positions relative to the silicate groups in clays. As a result the negative layer charge is concentrated on the proton-bearing oxygens rather than spread over the many silicate oxygens in the clay interlayer boundary. Although the layers are held together only by van der Waals forces, the interlayer distance is small and the bottlenecks provide just enough space for an unhydrated K^+ to diffuse into the interlamellar spacing. Thus, the crystals exhibit sieving behavior in acid solutions, and ions larger than K^+ are exchanged at an appreciable rate only in alkaline solution. Under these conditions sufficient protons on the layers are neutralized to allow swelling of the layers to admit larger ions.[26,27]

Exchange takes place in the crystals by diffusion of ions from the outer surface inward with advancing phase boundary. The layers expand to accomodate not only the ions but waters of hydration. Until the exchange process is complete, each particle or crystallite contains two phases, the original proton phase in the inner region and the cationic phase in the outer regions of the crystallite. Alberti[148] has developed a pictorial description of this phenomenon. This is illustrated in Figure 13. The wedge-shaped region connecting the inner proton region and the outer cation region contains both counterdiffusing ions. That the two phases coexist in the same particles was shown by heating the partially exchanged crystallites to 110–120 °C. At a level of 25% exchange of Na^+ in zirconium phosphate, the phases present are $ZrNaH(PO_4)_2 \cdot 5H_2O$ and $Zr(HPO_4)_2 \cdot H_2O$. After heating, the sodium ion redistributes itself to form two new phases:[150] $ZrNa_{0.2}H_{1.8}(PO_4)_2$ and $ZrNa_{0.8}H_{1.2}$-
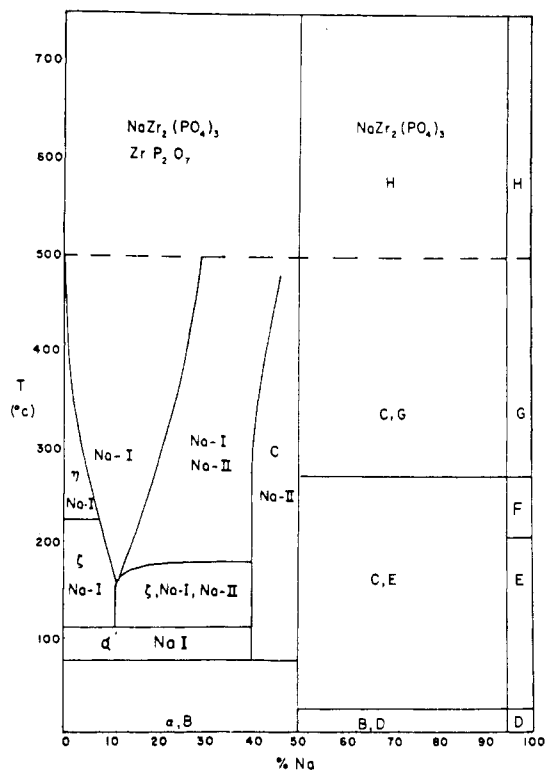

Figure 14. Phases formed by sodium-exchanged α-zirconium phosphate. (From ref 145, with permission.)

TABLE 6. Identification of the Phases in Figure 14[a]

designation	compos of phase	interlayer spacing, Å
A	$ZrNaH(PO_4)_2 \cdot 5H_2O$	11.8
B	$ZrNaH(PO_4)_2 \cdot H_2O$	7.9
C	$ZrNaH(PO_4)_2$	7.3
D	$Zr(NaPO_4)_2 \cdot 3H_2O$	9.8
E	$Zr(NaPO_4)_2 \cdot H_2O$	8.4
F	$Zr(NaPO_4)_2$	8.4
G	$Zr(NaPO_4)_2$	7.6
H	$Zr(NaPO_4)_2$	7.6
Na-I	$ZrNa_{0.2}H_{1.8}(PO_4)_2$	6.86
Na-II	$ZrNa_{0.8}H_{1.2}(PO_4)_2$	7.2
ζ-ZrP	$Zr(HPO_4)_2$	7.41
η-ZrP	$Zr(HPO_4)_2$	7.15

[a] From ref 145, with permission.

$(PO_4)_2$ in the correct proportions determined by the sodium ion content. The same type of redistribution occurs with amine intercalates which are not fully intercalated. Regions with more amine in contact with a region containing less or no amine, as determined by the interlayer spacings of the phases, redistribute the amine to form a single phase on heating.[151] Counterdiffusion of the ions is not necessary as some regions near the crystal edges will always be free of the ingoing ions. Thus, we picture the ingoing ions as displacing those ahead of them into adjacent cavities in a concerted movement, with an equal number of displaced ions pushing those near the edge out into the solution.

2. Phase Changes of α-Layered M(IV) Phosphates

Not only are new phases obtained on exchange but the hydrated ion containing phases also dehydrate in stages when heated. We have already mentioned redistribution of ions on heating the partially exchanged sodium ion phase in the previous section. Figure 14 and Table 6 list all the phases formed in the zirconium

phosphate–sodium ion system.[145] Figure 14 is not an equilibrium diagram as the temperature ranges of stability for each phase were determined by TGA and X-ray patterns taken at room temperature. A more complete explanation of the phase diagram is given elsewhere.[145] However, we note here that the half-exchanged phase A, when heated to 500 °C, forms Na-$Zr_2(PO_4)_3$. This triphosphate is not a layered compound but has a three-dimensional framework structure and is the end member of the NASICON family of fast ion conductors (see Section V.A).[152]

Even more complicated behavior is exhibited by the fully exchanged phase D, $Zr(NaPO_4)_2 \cdot H_2O$, as evidenced by the reaction scheme in eq 10. Phases F, G, and H

$$D \xrightarrow{100\ °C} E \xrightarrow{200\ °C} F \xrightarrow{260\ °C} G \xrightarrow{800\ °C} H \xrightarrow{1100\ °C} NaZr_2(PO_4)_3 + I \quad (10)$$
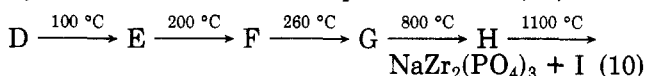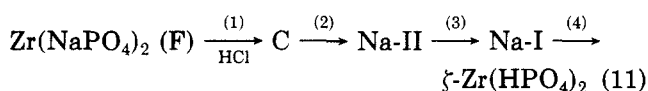
are anhydrous and retain a layered structure. However, phase I was recently shown[153-156] to be a solid solution of composition $Na_{1+4x}Zr_{2-x}(PO_4)_3$ with $0.95 \geq x \geq 0.88$. The relative proportions of the triphosphate and phase I depend upon the temperature of heating and time.[153]

Diagrams similar to those of Figure 14 have been published for Li^+, Mn^{2+}, Zn^{2+}, and Cu^{2+}.[157-159] These diagrams are especially interesting in the light of the discovery of fast ion conduction in compounds of the type $Na_{1+x}Zr_2Si_xP_{3-x}O_{12}$.[160,161] In the range $1.8 \leq x \leq 2.3$ such compositions exhibit conductivities of the order of $0.2\ \Omega^{-1}\ cm^{-1}$ at 300 °C.[160] One end member of the series is $NaZr_2(PO_4)_3$, which can be prepared by heating $ZrHNa(PO_4)_2$ to 500 °C.[27] The reaction in the case of Li^+ is more complicated. Heating $Zr(LiPO_4)_2$ to 600 °C yields a triphosphate-like phase which has not yet been clearly characterized. However, further heating to 1000–1100 °C converts it to $LiZr_2(PO_4)_3$ plus lithium phosphates. Refluxing in acid then dissolves the lithium phosphates and converts the lithium salt to H-$Zr_2(PO_4)_3$. Triphosphate phases are also obtained with divalent cations in a similar manner.[159,162] Many of the phases formed with divalent ions have not been well characterized, and no similar exploration of phases obtained with other group IV (groups 4 and 14) phosphates has yet been carried out. Study of such systems may provide a rich field for investigation of new ion exchangers, fast ion conductors, and new solid solution phases with interesting magnetic properties.

3. Gas–Solid and Fused-Salt Exchange Reactions

The α-layered compounds are able to undergo ion exchange with anhydrous salts.[143] For example, when NaCl is mixed with anhydrous α-ZrP and heated, HCl is evolved and sodium-exchanged phases are obtained. The phases formed are Na-I, Na-II, C, and F or G (Table 6), respectively, as the sodium ion content of the solid increases. The reactions are reversible and endothermic since hydrogen ion is selectivity favored by the exchanger. Similar reactions have been carried out with zeolites[144] and dry organic resins in the H form.

The rates of the reverse reactions of $Zr(NaPO_4)_2$ and HCl have been measured.[163] Phase F (Table 6) was the starting phase and the sequence of reactions is as follows:

$$Zr(NaPO_4)_2\ (F) \xrightarrow[HCl]{(1)} C \xrightarrow{(2)} Na\text{-}II \xrightarrow{(3)} Na\text{-}I \xrightarrow{(4)} \zeta\text{-}Zr(HPO_4)_2 \quad (11)$$

The reactions were diffusion controlled and could be fit by an equation for a spherical particle in a well-stirred fluid of limited volume. Diffusion coefficients are of the order of $10^{-12}\ cm^2/s$ in the temperature range 150–200 °C with activation energies of 10.3, 12.7, and 15.9 kcal/mol for reactions 1, 2, and 3, respectively. Extrapolation of the diffusion coefficient values to 25 °C yields coefficients of the order of $10^{-15}\ cm^2/s$. Thus, the gas–solid reactions are considerably slower than ion exchange reactions in solution, which typically have diffusion coefficients of the order of $10^{-12}\ cm^2/s$.[164]

Ion exchange in fused salts must be carried out with salt forms of the exchanger because release of protons would be followed by decomposition of the acid formed, or at high enough temperatures, decomposition of the exchanger. The ingoing ion usually forms a solid solution with a low solubility limit. When this limit is exceeded, a phase transformation occurs accompanied by a vertical line in the composition isotherm since two immiscible phases are now present. The isotherms are characterized by hysteresis loops when the ingoing ion expands the interlayer distance appreciably.[165,166] In the reverse reaction the smaller ion is able to accommodate itself in the space left vacant by the outgoing ion and no change in layer spacing occurs. In some cases the original phases (or the phase obtained from one complete exchange cycle) have a large enough interlayer spacing to accommodate all ions without appreciable interlayer spacing change. In such cases the exchange is reversible.

Proton conduction properties of the layered phosphates are presented in section V.C.2.a.

We have described in this section some aspects of the chemistry of the α-layered forms of metal phosphates. There are in fact several other layered types of group IV (groups 4 and 14) phosphates so that this class of compound is exceedingly large and varied.[1,39]

B. Group V (Groups 5 and 15) Phosphates

Recently, Piffard et al.[167] prepared $KSb(PO_4)_2$ by the solid-state reaction of a mixture of K_2CO_3, $NH_4H_2PO_4$, and Sb_2O_5. This compound has a layered structure in which the layer is very similar to that of α-zirconium phosphate. Extraction of the K^+ in strong acid yielded $HSb(PO_4)_2 \cdot xH_2O$,[168] which behaves as a strong acid and ion exchanger in much the same manner as zirconium phosphate, but with half the exchange capacity. A tantalum analogue $TaH(PO_4)_2$ was prepared earlier by the reaction of a Ta_2O_5 with H_3PO_4 at elevated temperatures.[169] Since tantalum compounds readily hydrolyze in basic solution, the alkali metal salts were prepared by a solid–solid reaction[170]

$$TaH(PO_4)_2 + MCl \xrightarrow{200\text{-}400\ °C} MTa(PO_4)_2 + HCl \quad (12)$$
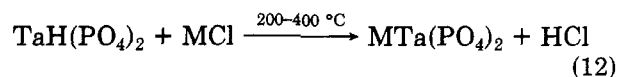
where M = Li^+, Na^+, K^+, Rb^+, and Cs^+. This reaction is very similar to those carried out with zirconium phosphate.[143] However, the Russian workers also used hydroxides in place of chlorides to facilitate the reaction.

Niobium phosphate, formed by dissolving Nb metal in HF followed by treatment with phosphoric acid, has a composition of $NbO(PO_4) \cdot 3H_2O$. It is a layered compound and able to intercalate amines.[171] In concen-

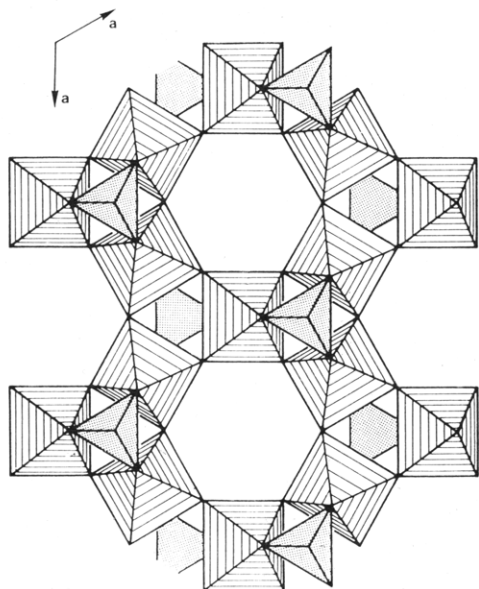**Figure 15.** Schematic representation of the layer structure in $H_3Sb_3P_2O_{14}$. (From ref 173, with permission.)

TABLE 7. Time (t) To Achieve $F(t)/F(\infty) = 0.95$ for Spherical Particles of Radius $r = 100\ \mu m^a$

D, cm² s⁻¹	10^{-5}	10^{-7}	10^{-9}	10^{-10}	10^{-11}	10^{-12}
t	2.5 s	4.2 min	6.9 h	69 h	29 days	290 days

examples	D, cm² s⁻¹	ΔH_m, kJ/mol
Na⁺ in molten NaCl (1300 K)	2.1×10^{-3}	30
Li⁺ in 1 M LiCl(aq) (300 K)	1.3×10^{-5}	
Na⁺/Li⁺ in Amberlite IR1 (300 K)	3.0×10^{-6}	
Na⁺ in Na β-alumina (300 K)	4.0×10^{-7}	16
Na⁺ in Na β-alumina (600 K)	1.8×10^{-6}	16
NH₄⁺/NEt₄⁺ in phenolsulfonic acid (300 K)	5.0×10^{-9}	21
Na⁺ in NaCl (intrinsic region, 900 K)	1.0×10^{10}	173
Na⁺ in NaCl (extrinsic region, 650 K)	1.0×10^{-12}	74
Na⁺/Tl⁺ in analcite (373 K)	4.5×10^{-13}	62

^{a} From ref 37, with permission.

trated phosphoric acid, the compound $NbO(PO_4)\cdot 3H_3PO_4\cdot5H_2O$ is obtained[172] in which H_3PO_4 is intercalated between $NbO(PO_4)$ layers. Exchange of phosphoric acid for other intercalates has been demonstrated.

A novel layered phosphatoantimonic acid of composition $H_3Sb_3P_2O_{14}\cdot xH_2O$ has also been prepared from the corresponding potassium salt by acid treatment.[173] It has a layered structure consisting of SbO_6 octahedra and PO_4 tetrahedra as shown in Figure 15. As in zirconium phosphate the phosphates are of the monohydrogen type, but there are only two phosphate groups and three hydrogens per formula. It is postulated that the third hydrogen atom is trapped on P–O–Sb or Sb–O–Sb framework oxygens. In spite of the difference in the hydrogen ion bonding, all the alkali metals except Li exhibit a single end point when $H_3Sb_3P_2O_{14}$ is titrated with the respective alkali metal hydroxides. Only LiOH forms both a two-thirds exchanged phase and a fully exchanged phase.

V. Fast Ion Conductors and Ion Exchange

Many of the ion exchangers discussed in the previous sections are ionic conductors, but very few exhibit fast ion conduction. Contrasting behavior is shown by fast ion conductors such as β-alumina and NASICON, which exchange ions but slowly from aqueous media and require forcing conditions for rapid exchange. As we shall see these conductors contain partially occupied, interconnected channels or cavities. In the case of ion transport, barriers exist to the movement of ions from one site to the next. The ion may be considered to be situated in a potential well and require energy, E_a, to surmount the barrier.[174] This barrier may take the form of narrow passageways from one cavity to another or movement from a lattice site to an interstitial site or created vacancy. Conduction requires single-ion movements, often in a concerted manner. In most organic resins counterdiffusion of ions can take place as the cavities in which ions reside can be quite large.[175] Solid electrolytes such as β-alumina or NASICON do not swell and ion transport must occur by a concerted or interstitialcy mechanism such as already suggested for zirconium phosphate. Thus, counterdiffusion of ions cannot occur in these materials and E_a values may be high for exchange at moderate temperatures. The barriers to exchange are overcome by using forcing conditions, such as exchange from fused salts, or under pressure, or heating in concentrated aqueous solutions were the exchange rate may then become quite appreciable. We have already seen that the exchange of protons for cations in many inorganic compounds requires strong acids at, or near, boiling temperatures.

Diffusion coefficients for ion conduction involve only single-ion coefficients, but those for ion exchange represent mixed or interdiffusion coefficients. England et al.[37] have calculated the time required to achieve 95% complete ion exchange for a range of diffusion coefficients. The results, including examples, are collected in Table 7. The implications of these data are clear; ion exchange is a necessary, but not sufficient condition for fast ion conduction.[37] However, even if the diffusion coefficients are small at room temperature they can be increased by several orders of magnitude at sufficiently elevated temperatures, thus producing extensive ion exchange even below the sintering temperature. However, the converse may not be true. Many compounds which exhibit facile exchange may still be poor conductors at elevated temperatures because the barriers to conduction remain. For example, many layered compounds which exchange readily at room temperature are poor ion conductors because the interlayer distance may decrease with increasing temperature, resulting in constricted passageways for the ions. These principles will be illustrated in what follows.

A. The NASICON System

NASICON (Na super ion conductor) is the acronym for the solid solution series of composition $Na_{1+x}Zr_2Si_xP_{3-x}O_{12}$. The structures of the phosphate end member ($x = 0$) and the silicate end member ($x = 3$) are known.[152,176] A portion of the phosphate structure is shown schematically in Figure 16. It is rhombohedral, $R\bar{3}c$, and consists of $Zr_2(PO_4)_3^-$ anions (shaded portion) in which the zirconium atoms are octahedrally coordinated by oxygen atoms from six different phosphate groups. The anions are then linked together in three dimensions by the remaining phosphate oxygens. This arrangement produces cavities (labeled A in Figure 16) in which the sodium ions reside.
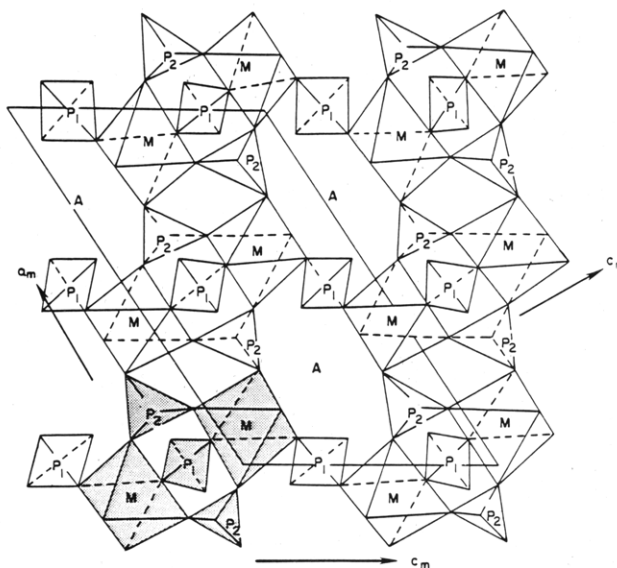
Figure 16. Projection onto the ac plane of the $NaZr_2(PO_4)_3$ structure showing cavity built up by linking of PO_4 and ZrO_6 groups. Shaded portion represents the $Zr_2(PO_4)_3$ ion. (From ref 160, with permission.)
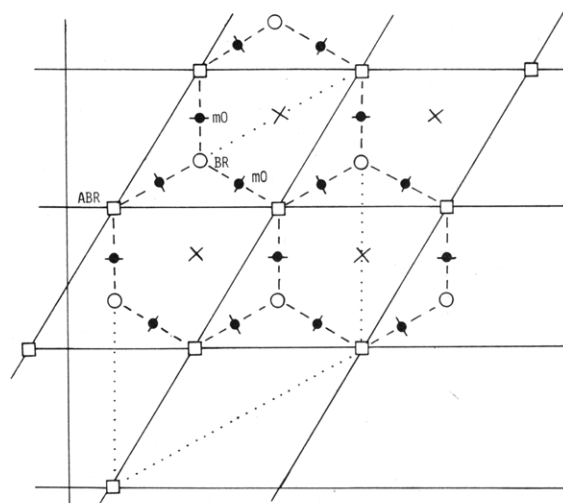

Figure 17. Schematic representation of the conduction plane in β-alumina showing the various ion sites. The oxygen atom positions are represented by crosses, the mid-oxygen (mO) sites by filled circles, Beevers–Ross (BR) sites by unfilled circles, and the anti Beevers–Ross (ABR) sites by squares. Heavy lines denote the unit cell and dotted lines the 3×3 supercell.

Figure 16 illustrates only half the unit cell. The other half is identical with the one shown but is shifted by $1/2c$. This creates three more cavities between the two halves which are empty. As the larger silicate groups replace phosphate, the additional sodium ions required to balance the charge fill up the cavities. At the same time the bottlenecks between cavities enlarge[177] so that E_a is reduced and the conductivity increases. Compositions for which $1.8 < x < 2.3$ are monoclinic and exhibit the highest conductivities.

The NASICON system has been examined mainly for its conduction properties, but Hong[160,178] found that both Ag^+ and Li^+ could be exchanged for Na^+ in $Na_3Zr_2Si_2PO_{12}$ in molten salts. Direct synthesis of Li^+ forms has not been achieved except for the end member ($x = 0$). The lithium ion phase, $Li_3Zr_2Si_2PO_{12}$, obtained by exchange, exhibited conductivities 4 orders of magnitude lower than the corresponding sodium ion phase. This was attributed to the small size of Li^+. It was suggested[178] that the high charge-to-radius value for this ion results in strong bonding to the framework oxygens. In contrast, sodium ions are located near the center of the cavities and thus are more weakly bonded. This idea gains some credence from the observation that $LiTi_2(PO_4)_3$ is a much better Li^+ conductor than is $LiZr(PO_4)_3$.[179] The unit cell dimensions for the titanium compounds are considerably smaller than those of the zirconium compound, indicative of smaller cavities with a greater chance of weaker, more uniform electrostatic bonding to oxygens forming the cavity. Both titanium and zirconium compounds readily exchange protons for Li^+ on treatment with acid,[180] indicating that the bottlenecks are not small enough to prevent relatively free movement of the ions. Still, the room temperature conductivity for $LiTi_2(PO_4)_3$ is low,[179] $\sigma_{25°C} = 7.9 \times 10^{-8}$ Ω^{-1} cm^{-1}. This is a case in point where ion exchange (of small ions) is facile, but conductivity is poor. However, at 300 °C, $\sigma = 5 \times 10^{-3}$ Ω^{-1} cm^{-1}. In contrast, Na^+ cannot be exchanged with H^+ in acid solution and the conductivity of the sodium phase is very low ($\sigma_{25°C} \simeq 10^{-10}$ Ω^{-1} cm^{-1}). However, exchange does occur with

$Na_3Zr_2Si_2PO_{12}$ in which the bottlenecks are much larger.[181] The protonated NASICONs exhibit reasonable conductivities at 300 °C ($\simeq 10^{-3}$–10^{-4} Ω^{-1} cm^{-1}).

Complete isotherms for Na^+–K^+ exchange in NASICONs with $x = 0$, 1, and 2 were determined[182] at 368 $\pm$ 4 °C by using mixed nitrates. In each case K^+ was preferred over Na^+. According to Eisenman's theory[183] (discussed in section VII.A), the larger ion is preferred when the ion is coordinated to several oxygen atoms (weak field) rather than strongly bonded to one negatively charged oxygen atom (strong field). The activity coefficients for the ions in the exchanged phases were roughly equal to those found in β-alumina.

Compounds with the NASICON or triphosphate framework structure constitute a very large class of compounds. Almost any four-valent cation can substitute for zirconium and partial isomorphous displacement of M^{4+} by M^{3+}, M^{2+}, or M^{5+} is possible.[184,185] In addition, compounds of the type $A_3M^{III}_2(PO_4)_3$ have been prepared[186] and studied in connection with structure and conduction properties. The ion exchange behavior of both groups of compounds has, however, been largely unexamined.

B. β-Aluminas

1. β-Alumina: Structure and Conductivity

β-Alumina is the name applied "historically" to a solid solution series of general formula $Na_{1+x}Al_{11}O_{17+x/2}$. The name is actually a misnomer since initially the presence of sodium ion in the compound was not recognized. Its structure consists of $Al_{11}O_{16}$ spinel blocks separated by planes of sodium and oxygen atoms. These oxygen atoms bridge aluminum atoms in adjacent spinel blocks. The space group is hexagonal $P6_3/mmc$ with $a \simeq 5.6$ Å and $c \simeq 22.5$ Å. The juxtaposition of Na^+ and planar oxygen atoms is shown in Figure 17, with the cation sites within the plane designated as Beevers–Ross (BR), antiBeevers–Ross (ABR), and mid-oxygen (mO) positions. X-ray and neutron diffraction studies show that the occupancy of the several sites varies with the type of ion, the magnitude of x, and temperature.[187] In the

interest of brevity a simplified and generalized description will be presented. In near-stoichiometric β-alumina (the stoichiometric composition is outside the range of homogeneity), the BR sites are filled.[188,189] The next site to be occupied is mO. Since the most common values of x range from 0.15 to 0.3, roughly one-sixth to one-third of the mid-oxygen sites are occupied. The presence of a cation near an occupied BR site causes the Na^+ there to relax away from this site to an mO site. This so-called interstitial pair, at the mid-oxygen positions, share a BR site, and this sharing lowers the potential barrier for ion motion from about 2 to 0.15 eV.[190] Ion motion is then thought to occur by an interstitialcy mechanism in which one ion moves into a BR site while the adjacent ion in an mO site hops across to another mO site near an occupied BR position. Thermal motion also causes increased disorder, and at elevated temperatures a liquid-like smearing out of ion density is observed.[174] Sodium ion conduction within the plane may be as high as 10^{-2} Ω^{-1} cm^{-1} at room temperature in single crystals.

2. β''-Alumina: Structure and Conductivity

In β''-alumina cations of lower charge such as Mg^{2+} or Li^+ replace some of the Al^{3+} in the spinel block. The value of x is typically 0.67. To accommodate this large excess of Na^+, the spinel blocks arrange themselves differently. In β-alumina, the conduction planes are mirror planes with trigonal-prismatic coordination of the sodium ions in the BR sites. However, in β''-alumina, the spinel blocks are shifted relative to each other such that both the BR and ABR sites are equivalent and tetrahedrally coordinated. The unit cell thus requires three spinel blocks with $c \simeq 33.75$ Å. The β''-arrangement of spinel blocks leaves more room in the conduction plane in the c direction so that ions can be slightly above or below the plane. Movement of ions within the plane is thereby facilitated. Conduction occurs by cation vacancy motion.

Potential energy models predict that the activation energy for a single sodium ion vacancy should be about 0.02 eV,[191] but at room temperature the value observed is about 0.33 eV. This large energy value is attributed to ion–ion correlations. Evidence from diffuse X-ray scattering[174,192] shows an ordering of the vacancies with a superlattice built on a cell of dimensions $3^{1/2}a \times 3^{1/2}a$, as shown in dotted outline in Figure 17. The ordered vacancies are trapped at these sites, requiring more energy to hop to a neighboring position than would be required if there were no superlattice ordering. Increased temperature causes a disordering of the superlattice and a decrease in E_a to near the calculated value.

3. Ion Exchange in β- and β''-Alumina

Perhaps the first reference to the ion exchange behavior of β-alumina is that of Toropov and Stukalova,[193] who prepared Ca^{2+}-, Sr^{2+}-, Ba^{2+}-, and Rb^+-exchanged phases from fused salts. Yao and Kummer[194] carried out an extensive examination of univalent and divalent exchange in Na-β-alumina. Exchange with univalent ions was found to proceed rapidly at about 300 °C in fused-salt media. Complete isotherms for a number of ions were determined and these are shown in Figure 18. The shape of the isotherms depends upon the anion
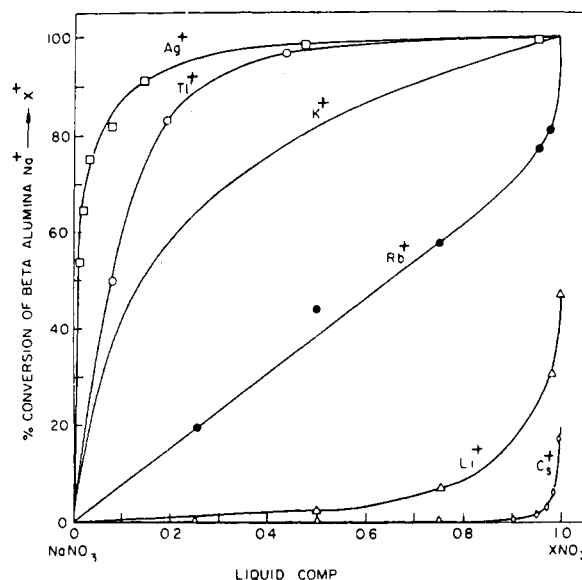

Figure 18. Equilibria between β-alumina and various binary nitrate melts containing $NaNO_3$ and another metal nitrate at 300–350 °C. (From ref 194, with permission.)

used in the salt bath as is shown by the following arguments:

The ion exchange reaction can be represented by

$$\overline{RNa^+} + (MX)_l \rightleftharpoons \overline{RM^+} + (NaX)_l \qquad (13)$$

where R represents the β-alumina framework, and the bars indicate the solid exchanger phase. For this reaction

$$\Delta G° = \Delta G°_f(RM) - \Delta G°_f(RNa) + \Delta G°_f(NaX)_l - \Delta G°_f(MX)_l \qquad (14)$$

Since no anions enter the solid phase, only the last two free energy terms change with change in the anion X. In some cases these changes are large and can make either Na^+ or M^+ the preferred ion. In chloride melts K^+ was preferred, but in iodide melts, Na^+ was the preferred ion.[194] An extreme example is that of Li^+, which is greatly preferred by the melt so that very little is exchanged. However, if Ag^+-β-alumina is substituted for the sodium phase in a chloride melt, total exchange occurs due to the low solubility of AgCl in the melt.

Self-diffusion coefficients (D_i) for univalent ions were measured by using radiotracers. At 350 °C the magnitudes of D_i ranged from 10^{-5} cm^2 s^{-1} for Na^+ to 10^{-7} cm^2 s^{-1} for Rb^+ with the order $Na^+ > Ag^+ > Li^+ \simeq K^+ > Rb^+$. However, rates of ion exchange depend on interdiffusion coefficients. For interdiffusion of alkali metal ions in β-alumina it was found that, for K^+ exchange with Na-β-alumina, the interdiffusion coefficient increases with K^+ uptake, while if Na^+ exchanges for K^+ the opposite is true. These changes of interdiffusion coefficients with composition are qualitatively in the right direction (see eq 33). However, exchange rates in β-alumina are also influenced by correlation effects[195] and the change in dimensions of the conduction planes. Both these factors require further examination.

Yao and Kummer[194] also found that β-alumina was a poor exchanger for divalent ions as they required temperatures of 600 °C or greater to achieve partial exchange. In contrast, β''-alumina was found to readily exchange a variety of divalent ions.[196] For Sr^{2+} uptake the diffusion coefficient determined from the ion ex-

change rate was found to predict conductivities with a fair degree of accuracy. Conductivities at 40 °C are of the order of 10^{-6} Ω^{-1} cm^{-1} while at 300 °C they are 10^{-2} Ω^{-1} cm^{-1}. Surprisingly, Pb^{2+} exhibited much higher conductivities approaching those of Na^+-β''-alumina. It was also found that additions of small amounts of Ca^{2+} to Na^+-β''-alumina lowered the conductivity significantly, i.e., close to the conductivity of pure Ca^{2+}-β-alumina.

Farrington and Dunn[196] attribute the differences in ion exchange and conductivity behavior of divalent ions in β-alumina and β''-alumina to the different conduction mechanisms. In β-alumina the intertialcy mechanism requires that both BR and mO sites be occupied to lower the barrier to diffusion. In divalent ion phases there are fewer cations than BR sites, so all the cations are presumably trapped in deep potential wells at the Beevers–Ross sites. In β''-alumina this smaller number of cations results in more vacancies. Since the BR and ABR sites are equivalent in β''-alumina, approximately 42% of the sites are filled and 58% are empty, allowing for high conductivity by the vacancy mechanism. More recent structural work[197-199] has shown great variation in site occupancy. With Ba^{2+} all the ions are in BR sites, while with Pb^{2+}, 90% of the ions are in the BR sites and 10% in mO sites, and with other ions (Sr^{2+}, Cd^{2+}, Mn^{2+}), more than 50% of the ions are in mO sites. In addition, the bridging oxygen shows considerable variation in its position between the spinel blocks, depending upon site occupancies of the cations.

Several trivalent lanthanide β''-aluminas have also been prepared[200,201] as have mixed-valent forms.[202] The lanthanide phases all have a majority of the trivalent cations situated at mid-oxygen sites,[202,203] with only minor occupancy of the BR sites. Apparently, many of the multivalent phases are characterized by ordering of the cations to produce superstructures.[199] Even three-dimensional long-range order has been noted in Cd^{2+}-β-alumina and lanthanide phases. These structural studies indicate that a variety of different ion positionings are possible for multivalent ions. While these positionings have only a minor effect on conductivity, they exert a large influence on optical properties.[202] On the other hand, site occupancies of mixed-ion β''-aluminas have a major effect on their conductivity.

The extensive ion exchange chemistry of β- and β''-alumina allows a great variety of different cation forms to be prepared. This variety affords the opportunity to study the effect of ion environments on transport and other properties in a systematic fashion. The research effort needs to include ion exchange studies along with conductivity and structural information to correlate theory with experimental data.[204]

C. Proton Conductors

In recent years there has been an intensification of research aimed at discovering new proton conductors and the mechanisms of conduction in these compounds. This renewed activity has been driven by the potential use of such compounds in fuel cells, sensors, water electrolysis units, and other electrochemical devices. Research on proton conduction up to 1973 has been reviewed by Glasser.[205] More recent collections of papers may be found in the proceedings of international

TABLE 8. Values of Proton Conductivity in Some Solid Electrolytes[a]

materials	conductivity, Ω^{-1} cm^{-1}	temp, K
$H_3PMo_{12}O_{40}\cdot29H_2O$	1.8×10^{-1}	298
$H_3PW_{12}O_{40}\cdot29H_2O$	1.7×10^{-1}	298
$HUO_2PO_4\cdot4H_2O$	4×10^{-3}	290
$HUO_2AsO_4\cdot4H_2O$	6×10^{-3}	310
$H_8UO_2(IO_6)_2\cdot4H_2O$	7×10^{-3}	293
H_3OClO_4	3×10^{-4}	298
$Sb_2O_5\cdot4H_2O$	3×10^{-4}	293
$SnO_2\cdot3H_2O$	2×10^{-4}	293
$ZrO_2\cdot2.3H_2O$	3×10^{-5}	293
H^+-montmorillonite	$(1-4) \times 10^{-4}$	290
H-Al-montmorillonite	10^{-4}–10^{-2}	290
hydrated hydronium β''-alumina	5×10^{-3}	298
NH_4^+-β-alumina	$\simeq 10^{-3}$	523
$NH_4^+/H(H_2O)_x^+$-β''-alumina	$\simeq 10^{-4}$	298
$C_6H_{12}N_2\cdot1.5H_2SO_4$	$\simeq 10^{-6}$	298
$C_6H_{12}N_4\cdot2H_2SO_4$	$\simeq 10^{-7}$	298

[a] Adapted from: Huggins, R. A. In *Materials for Advanced Batteries, Proceedings of NATO Symposium on Materials for Advanced Batteries, Aussois, France, 1979*; Murphy, D. W., Ed.; Plenum Press: New York, 1980.

conferences.[206-209] Huggins[210] summarized the situation to 1979 and his list of proton conductors is given in Table 8. A major shortcoming of these compounds is that they require water or ammonium ion species for fast ion conduction. When this water or proton carrier is lost, the conductivity is decreased by several orders of magnitude. This behavior points to a Grotthus mechanism, which was described in sections II.A.2 and II.B.3 in connection with proton conduction in hydrous oxides. A further brief discussion of proton conduction mechanisms is given below.

1. Proton Conduction Mechanisms

Proposed mechanisms for proton diffusion include, in addition to the Grotthus mechanism, complex ion diffusion (H_3O^+, NH_4^+) or vehicle mechanisms[211] and proton hopping or tunneling. The Grotthus mechanism requires close proximity of water molecules which are firmly held but able to rotate. Compounds with lesser amounts of water would be expected to conduct by the vehicle mechanism in which a nucleophilic group such as H_2O or NH_3 acts as a carrier for the proton. Kreuer et al.[211] have pointed out that the activation energy for water translation in hydrogen uranyl phosphate (HUP) and proton conduction in this compound are similar in magnitude (0.8 and 0.64 eV, respectively) whereas the activation energy for water rotation is 0.27 eV. Comparison of activation energies led them to conclude that the diffusion mechanism is operative in HUP. We would then expect such a mechanism to be operative with framework hydrates in which the acidity is high enough that the cavities are essentially occupied by H_3O^+ or similar protonated molecules but little additional water is present.

In both particle and framework hydrates, the loss of all or most of the nucleophiles forces the proton to take positions on the lattice oxygens. Proton transport then takes place by hopping along lattice sites. This process requires a constant breaking and making of bonds with a concomitant high activation energy. Proton conduction is thus slow. Compounds with very high Brønsted acidity facilitate this mechanism. For acids of the type H_xMO_y, the acid strength increases as one

TABLE 9. Specific Conductance of α-ZrP Samples Obtained by Different Methods of Preparation and Ordered According to Their Degree of Crystallinity

sample no.	prep method	specific conductance, Ω^{-1} cm^{-1}
1	precipitation at room temperature, amorphous[a]	8.4×10^{-3}
2	precipitation at room temperature, amorphous	3.5×10^{-3}
3	refluxing method (7:43), semicrystalline	6.6×10^{-4}
4	refluxing method (10:100), crystalline	9.4×10^{-5}
5	refluxing method (12:500), crystalline	3.7×10^{-5}
6	slow precipitation from HF solution, crystalline	3.0×10^{-5}

[a] The specific conductance was measured by an isoconductance method at 25 °C. The values for samples 1 and 2 strongly depend upon the conditions of preparation.[212]

proceeds up a group or to the right within a row of the periodic table. Some examples are presented in the next few sections.

2. Layered Phosphates

(a) Zirconium Phosphate. Almost all good proton conductors are good ion exchangers, which is in line with their high Brønsted acidity. Both zirconium phosphate and HUP fit this description. In considering the proton conduction properties of α-zirconium phosphate it is necessary to recall that this compound can be prepared as a gel, as crystals, and in all intermediate stages between these extremes.[1] The specific conductance as a function of the degree of crystallinity is shown in Table 9. It is seen that the less crystalline the sample, the higher the conductivity.[212] Alberti et al.[213] were able to show that the surface conducts protons 1000 times faster than the interior. The activation energy for surface conduction was 0.17 eV, whereas for conduction in the interior E_a was found to be 0.65 eV.[214] In α-zirconium phosphate the water molecule is hydrogen bonded by two of the phosphate protons and forms a hydrogen bond as donor to a third phosphate group.[25,26] There is no evidence for the presence of hydronium ions. Thus, conduction in the interior of the crystal must occur by a modified vehicle mechanism as rotation of the water molecule is difficult. It is proposed that the higher surface conductivity is due to the ability of water located there to rotate and participate in Grotthus-type transport aided by water sorbed on the surface.[214] As the crystallinity of the sample is decreased, its surface area increases,[215] accounting for the observed increase in conductivity. In the case of amorphous zirconium phosphate, swelling occurs in water and hydronium ions may form,[39] allowing for a Grotthus transport mechanism. Complete removal of water requires the proton to hop, and accordingly the conductivity decreases to $\simeq 10^{-7}$ Ω^{-1} cm^{-1} at 200 °C, increasing to 10^{-6} Ω^{-1} cm^{-1} at 300 °C.[216] Alberti et al.[217] were able to delaminate zirconium phosphate by an intercalation–deintercalation reaction and prepare thin sheets from an aqueous suspension of the pellicles. The conductivity parallel to the sheets was determined to be approximately 10^{-4} Ω^{-1} cm^{-1} at 300 °C and $\simeq 10^{-7}$ Ω^{-1} cm^{-1} perpendicular to the sheets. This parallel conductivity is 2 orders of magnitude greater than $\sigma_{300°C}$ for a powder compact as reported by Jerus and Clearfield.[216] Thus, by further manipulation of the pellicles

it may be possible to increase the conductivity to near the maximum theoretical values obtainable for a proton-hopping mechanism.

(b) Hydrogen Uranyl Phosphates. Hydrogen uranyl phosphate, $UO_2(HPO_4)\cdot 4H_2O$, has a layered structure in which uranyl ions are bridged by phosphate groups. The water molecules are arranged in squares with a staggered double layer of such squares in the interlamellar space. HUP has been shown to exhibit exceptionally high conductivities ($\simeq 0.4 \times 10^{-2}$ Ω^{-1} cm^{-1}) at 17 °C. A brief summary of its structure, physical properties, and ion exchange behavior has been published recently.[1] The very high room temperature conductivity and intricate water structure make HUP an ideal subject for diffusional and conductivity studies. In addition, HUP can easily be fabricated into dense disks or films for use in electrochemical devices.[218-220] England et al.[37] considered HUP to be a particle hydrate with the water held loosely enough to favor a Grotthus mechanism. Evidence for water rotation was obtained earlier by Childs et al.,[221] who also suggested a Grotthus-type mechanism. However, neutron diffraction[222] and NMR diffusivity studies[223] indicated different mechanisms for diffusion and conduction. These results led Kreuer et al.[211] to propose a vehicle mechanism for conduction. This question was further investigated by Tsai et al.[224] by pulsed field gradient NMR. They concluded that diffusion and conductivity do take place by the same mechanism but leave open to question the exact mechanism, whether Grotthus or vehicle.

A similar uncertainty exists concerning the mechanism of ion exchange behavior. The rate of exchange as measured by proton release is very fast for Na$^+$, K$^+$, and Rb$^+$ but slower for Cs$^+$ and NH$_4^+$. Higher valent ions require 40 min or more to achieve equilibrium.[225] Vesely et al. concluded that exchange occurred by a solution–reprecipitation mechanism.[226,227] However, Howe pointed out[1] that a normal interdiffusion mechanism cannot be ruled out on kinetic grounds. Calculated self-diffusion coefficients showed that univalent ions move rapidly enough in HUP to account for the observed kinetics.

HUP would be ideal for use as an ionic conductor were it not for its loss of water at relatively low temperatures with an attendant large decrease in conductivity.

3. Protonic β/β''-Alumina

Two reviews of this topic have appeared in the recent literature.[228,229] Protonated forms of β-alumina may be prepared by direct reaction with acids, deamination of the ammonium ion phase, or hydrogen reduction of Ag$^+$-β-alumina. The hydronium phase has been reported to have widely different conductivities,[229] but the differences may be due to compositional or structural variations which were not resolved. In any event the conductivities are generally low. It has been suggested that a Grotthus mechanism is operative below 150 °C through an intricate hydrogen bond network, and above this temperature, a vehicle diffusion mechanism is thought to be operative.

In contrast to β-alumina, hydronium β''-alumina has a conductivity which has variously been reported as high as 10^{-2} or as low as 10^{-6} Ω^{-1} cm^{-1} at 25 °C. High
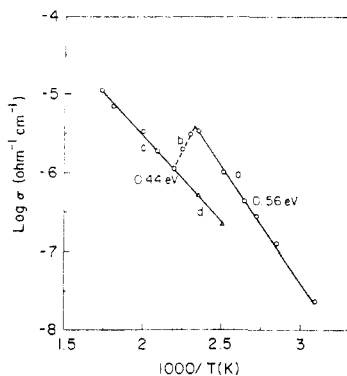
Figure 19. Plot of log σ as a function of $1/T$ for $(H_3O)Zr_2(PO_4)_3$. (From ref 232, with permission.)

Figure 20. Schematic structure of $H_3PMo_{12}O_{40}\cdot nH_2O$. (From ref 33, with permission.)

conductivities may be associated with the fact that the hydronium ion phase contains more water than protons; i.e., the composition reported is $H_{1.74}Mg_{0.74}Al_{10.26}O_{17}\cdot 2.33H_2O$. Vibrational spectroscopic studies have been interpreted on the basis that a mixture of H_3O^+ and $H_5O_2^+$ species are present. Dehydration occurs in stages but there is disagreement as to the actual composition formed. Furthermore, structural studies are also incomplete and in some cases difficult to interpret due to disorder effects. An interesting observation is the high conductivities observed in ammonium and mixed ammonium–hydronium phases. It is felt that the NH_4^+ ion can participate fully in Grotthus or vehicle conduction processes.

Although a great deal of work has now been done on the protonated β/β''-aluminas, they are still not well characterized or understood. This undoubtedly results from the wide range of compositions possible, the nonuniformity of the host lattice, and difficulty in interpreting data obtained from a single characterization technique. Thus, more comprehensive studies on a few samples are required for a better understanding of the protonic phases.

4. Protonated NASICONs

$HZr_2(PO_4)_3$ has been prepared by thermal decomposition of $NH_4Zr_2(PO_4)_3$[230,231] or treatment of $LiZr_2(PO_4)_3$ with dilute acid.[180] Clearfield et al.[230] were able to prepare the ammonium phase by hydrothermal treatment of α-zirconium phosphate with NH_4Cl at 250 °C. Temperatures above 450 °C are required to remove the NH_3, and the resultant $HZr_2(PO_4)_3$ is stable to 700 °C. Refluxing $HZr_2(PO_4)_3$ for 10–12 h in water converts it to $(H_3O^+)Zr_2(PO_4)_3$. Conductivity data for both the hydronium and protonated forms are shown in Figure 19.[232] Surprisingly, $HZr_2(PO_4)_3$ exchanges protons for Li^+ and Na^+ rapidly in aqueous media at room temperature.[231] Larger ions exchange much more slowly and incompletely. Apparently, exchange is hindered by the size of the bottlenecks, which do not permit Na^+ to be exchanged for H_3O^+ in $NaZr_2(PO_4)_3$. However, the passageways must be slightly larger in H_3O^+ since the reverse exchange (Na^+ replacing H_3O^+) takes place with ease. This hypothesis is supported by the fact that the hydronium phase has a larger unit cell than $NaZr_2(PO_4)_3$. One may also argue from a thermodynamic viewpoint that the sodium ion phase is greatly preferred to the hydronium phase. However, the exchange experiments were run under nonequilibrium conditions where the aqueous HCl solution was flowing over the
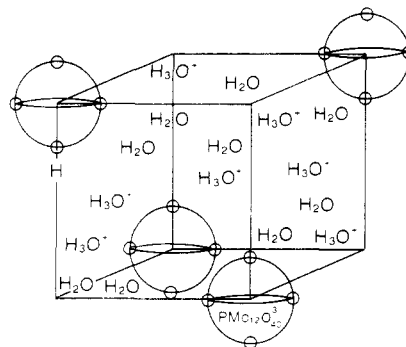
solid $NaZr_2(PO_4)_3$. Thus even if the sodium ion phase is the more stable one, some exchange (other than on the surface) should have occurred. However, if a pathway for exchange is not available, then no exchange will occur irrespective of the thermodynamics of the situation. Rietveld refinement of neutron time-of-flight powder diffraction data, taken at 15 K, showed that both NH_4^+ and H_3O^+ occupy the type I cavities only.[233] Both species are hydrogen bonded to the oxygens outlining the cavities and are larger than the passageways leading into the empty type II cavities. These factors could account for the low conductivity of the hydronium ion phase, but caution in this interpretation is necessary since the passageways may be considerably larger at 100 °C.

Conduction in $HZr_2(PO_4)_3$ must occur by proton hopping. Only a slight improvement in the conductivity is observed for $(H_3O^+)Zr_2(PO_4)_3$. It is suggested that conduction in this compound occurs by hydronium ion drift. The fact that three-fourths of the cavities are empty would preclude a Grotthus-type mechanism. However, one might imagine that the conductivity would be much improved in $(H_3O^+)_3Zr_2Si_2PO_{12}$ since the bottlenecks would be enlarged and only one-fourth of the sites would be empty. Preliminary data[181] indicate that this supposition is correct.

5. Miscellaneous Conductors

Heteropolyacids such as $H_3Mo_{12}PO_{40}\cdot 29H_2O$ and $H_3W_{12}PO_{40}\cdot 29H_2O$ are among the best proton-conducting solids known ($\sim 0.2\ \Omega^{-1}\ cm^{-1}$ at 25 °C).[181,234] A schematic representation of the structure due to England et al.[37] is shown in Figure 20. The $(PMo_{12}O_{40})^{3-}$ anions are almost spherical with an outer surface of strongly bonded oxygens. The high formal charge of Mo^{6+} would tend to polarize the electronic clouds of the oxygen atoms inward toward the Mo atoms, reducing the strength of the O–H bond. Therefore, the hydrogen ions are probably present as H_3O^+, and the compound may be considered to be a particle hydrate.[37]

Defect perovskites such as lanthanum aluminate and yttrate, for which some lower valent ion has been substituted for the trivalent ion, have been shown to conduct protons at elevated temperatures.[235] Hydrogen ions are supplied by the presence of a hydrogen atmosphere. In $La_{1-x}Ca_xYO_{3-x/2}$, the conductivity was found to increase with increased values of x up to 0.2. Substitution of the lower valent ion for La^{3+} creates oxygen vacancies which also allow transport of O^{2-} in an oxygen atmosphere. Conduction has been attributed to va-

cancy formation as shown in eq 15, where $\square_{O^{2-}}$ is an

$$(1 - x)LaO_{1.5} + {}^{1}/_{2}Y_2O_3 + xCaO \rightarrow$$
$$La_{1-x}Ca_xYO_{3-x/2} + (x/2)\square_{O^{2-}} \quad (15)$$

oxide ion vacancy. In an oxygen atmosphere the oxide ion vacancy will react with O_2 to produce an electron hole (eq 16)

$$^{1}/_{2}O_2 + \square_{O^{2-}} \rightarrow + 2h^+ + O^{2-} \quad (16)$$
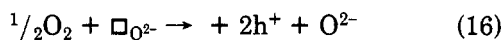
and thus exhibit p-type semiconduction. where h^+ represents an electron hole. In an H_2 atmosphere interstitial protons are thought to be generated by interaction of hydrogen with the holes (eq 17).[235,236] Applications of defect perovskites as solid electrolytes in fuel cells, steam electrolysis, and humidity sensors is in progress.

$$^{1}/_{2}H_2 + h^+ \rightleftharpoons H^+ \quad (17)$$
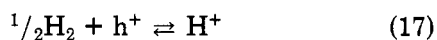
It should also be mentioned here that cation forms of β-alumina also have been shown to conduct protons[237,238] and that the writer has observed a similar phenomenon with NASICON.[239] These observations bear further examination.

VI. Anion Exchangers

We have previously (section II.A) discussed the anion exchange capability of particle hydrates. Another large class of anion exchangers is the hydrotalcite clays and their synthetic analogues.[240] These compounds have the general formulas $[M^{II}_3M^{III}(OH)_8]^+X_{1/z}{}^{z-}$ or $[M^{II}_2M^{III}(OH)_6]^+X_{1/z}{}^{z-}$. The mineral hydrotalcite is $Mg_6Al_2(OH)_{16}CO_3\cdot4H_2O$, in which Al^{3+} replaces some of the Mg^{2+} ions in a brucite-type layered structure. The anions reside between the layers and the Mg:Al ratio can vary over wide limits. Other divalent cations which form similar structures include Fe^{2+}, Co^{2+}, Ni^{2+}, Cu^{2+}, and Zn^{2+} while Fe^{3+} and Cr^{3+} may replace aluminum. Biloen et al. have shown[241] that monovalent ions such as lithium can form similar layered species of composition $[Al_2Li(OH)_6]^+$. A great variety of anions have been incoroporated in the interlamellar spaces, but $CO_3{}^{2-}$ is strongly preferred in alkaline solution.

Synthetic products are prepared by coprecipitating the two metals as hydroxides with a dilute NaOH–Na_2CO_3 solution and heating at 65–200 °C for several hours in the mother liquor. Carbonate ion is difficult to displace but an efficient procedure involves titrating a weighed amount of hydrotalcite with dilute acid until all the carbonate ion is released as carbon dioxide.[242] Once the carbonate ion is replaced by a large univalent ion such as $ClO_4{}^-$ or Cl^-, exchange of other anions is much facilitated. In fact, large anions such as carboxylic acids can then be incorporated in the interlamellar space.[243]

Heating the hydrotalcites above 600 °C converts them to very active mixed oxides which exhibit catalytic properties. The use of hydrotalcites as catalysts, anion exchangers, especially for sorption of environmentally undesirable anions, and medicinal agents are being explored.[239]

VII. Some Theoretical Considerations

We have seen in this review that a vast range of compounds is now known to exhibit ion exchange

properties and many of these are also fast ion conductors. In this section we consider those factors which determine whether ion exchange will take place and the extent of exchange. In this connection we need to discuss thermodynamic, kinetic, and structural factors.

A. Thermodynamics of Ion Exchange

Consider the general ion exchange reaction

$$\overline{R^-A^+} + B^+ \rightleftharpoons \overline{R^-B^+} + A^+ \quad (18)$$
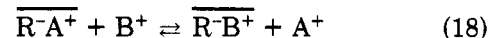
where R^- stands for the ion exchanger matrix and A^+ and B^+ are the exchanging ions, which for simplicity are considered to be univalent. Barred quantities represent the exchanger phase. The thermodynamic equilibrium constant for the reaction represented by eq 18 is

$$K_T = \frac{a_{A^+}\bar{a}_{B^+}}{a_{B^+}\bar{a}_{A^+}} \quad (19)$$

a_{A^+} and a_{B^+} are the activities of these ions in the exchange medium, which could be aqueous, a variety of mixed and nonaqueous solvents, or a fused-salt bath. Activity coefficients for the ions in the exchanging medium are generally known or can readily be determined, whereas activity coefficients for the ions in the exchanger phase are not. However, by following the procedure of Gaines and Thomas,[244] we can obtain K_T from the exchange isotherms.

$$K_T = K_R(\bar{f}_{B^+}/\bar{f}_{A^+}) \quad (20)$$

where

$$K_R = \frac{a_{A^+}\bar{X}_{B^+}}{a_{B^+}\bar{X}_{A^+}} \quad (21)$$

K_R is the correlated rational selectivity constant, $\bar{f}_{A^+}$ and $\bar{f}_{B^+}$ are the activity coefficients of the ions in the exchanger, and $\bar{X}_{A^+}$ and $\bar{X}_{B^+}$ are the mole fractions of the exchanging ions in the exchanger phase. Gaines and Thomas showed that (neglecting any solvent transfer)

$$\log K_T = \int_0^1 \log K_R \, d\bar{X}_{B^+} \quad (22)$$

Thus, by plotting $\log K_R$ as a function of $\bar{X}_{A^+}$ over the entire composition range from $\overline{RA}$ to $\overline{RB}$, one may extract the value of K_T from the area under the curve.

This treatment, while extremely useful, gives us little insight into the exchange process itself. Therefore, nonthermodynamically rigorous models have been developed to provide the required understanding. For our purposes the most useful model is that due to Eisenman.[183]

Suppose a monovalent ion to be taken from the bulk of a dilute solution and brought into contact with the fixed ionic grouping (of opposite charge) of the ion exchanger. Two types of interaction energies are involved in such a change: (1) the electrostatic interaction between the fixed grouping and the counterions (the exchanging ions) and (2) the free energies involved in the changes in hydration of the counterions and the fixed grouping.

Eisenman treated the fixed grouping and the counterion as being point charges each at the center of an incompressible sphere. If the fixed grouping is anionic with a radius r_f, then the electrostatic energy arising from its interaction with a cation A^+ of radius r_{A^+} is

$$\frac{e^2}{r_{f^-} + r_{A^+}} \tag{23}$$

where e is electronic charge. Similarly, the interaction of the fixed grouping with cation B^+ would give rise to the electrostatic energy

$$\frac{e^2}{r_{f^2} + r_{B^+}} \tag{24}$$

and the change in free energy for the exchange reaction, eq 18, is then

$$\Delta G^\circ_E = \frac{e_2}{r_{f^-} + r_{A^+}} - \frac{e^2}{r_{f^-} + f_{B^+}} \tag{25}$$

Eisenman assumed that the free energy changes resulting from changes in hydration are closely related to the standard free energies of hydration of the ionic groups. Thus, the free energy change due to hydration changes occurring when B^+ is brought from the solution into the exchanger is $\Delta G_{f^-} + \Delta G_{B^+}$, where ΔG_{f^-} and ΔG_{B^+} are the free energies of hydration of the fixed group and cation B^+, respectively. Similarly, when cation A^+ leaves the exchanger and enters the solution the free energy change due to hydration effects is $-(\Delta G_{f^-} + \Delta G_{A^+})$. Thus, the net free energy change for hydration (assuming no hydration change inside the exchanger) is

$$\Delta G^\circ_h = \Delta G_{B^+} - \Delta G_{A^+} = -(\Delta G_{A^+} - \Delta G_{B^+}) \tag{26}$$

and the overall free energy change for the reaction is

$$\Delta G^\circ_{B/A} = \left(\frac{e^2}{r_{f^-} + r_{A^+}} - \frac{e^2}{r_{f^-} + r_{B^+}} \right) - (\Delta G_{A^+} - \Delta G_{B^+}) \tag{27}$$

The equilibrium constant for the exchange reaction is related to this free energy by

$$\Delta G^\circ_{B/A} = -RT \ln K_T \tag{28}$$

Thus, from a knowledge of ionic radii and free energies of hydration, Eisenman was able to calculate selectivities for alkali metal cations as a function of r_f. It was necessary to make assumptions as to whether the negative charges on the exchanger fixed groups are concentrated at single-atom sites (strong field) or distributed among several atoms (weak field). Eisenman's calculations predicted 11 possible sequences for alkali metal ions and showed how selectivity reversals arise. The theory was highly successful in predicting the selectivities of glasses as a function of their composition (which determined the nature of the fixed ionic groups). This in turn proved of great value in the theory of glass electrode and single ion electrode behavior.[245] The general agreement between the theoretical predictions and experimental results indicates that Eisenman's theory is basically sound. In applying the theory to a broad spectrum of ion exchange materials, it is reasonable to expect that additional factors peculiar to individual ion exchange systems, particularly biological systems, may have to be introduced. Before this can be done with any certainty it is essential to develop, in more precise terms, the role played by Coulombic interactions and hydration effects. In addition the magnitude of the Coulombic effect has not been measured directly and therefore is not known with precision. However, Clearfield et al.[246] were able to deter-

mine, from gas–solid reactions involving exchange reactions of the type

$$Zr(NaPO_4)_2 + (HCl)_g \rightleftharpoons Zr(HPO_4)_2 + 2NaCl \tag{29}$$
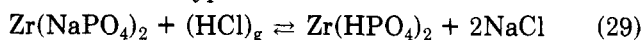
that indeed the electrostatic effect predicted the correct selectivity sequence. No hydration effects were involved in these reactions.

If now we substitute a fused-salt medium for the aqueous electrolyte solution, then the hydration effect must be replaced by one entailing the coordination of the mobile cations in the fused salt. As a first assumption we consider that the cations are surrounded by anions much as in their crystal lattices. Therefore, a good approximation is to use lattice energies modified by using an average first-shell coordination number rather than the Madelung constant. For two ions with the same charge and coordination number, the smaller ion would require more energy to give up its position in the melt than would be supplied by the incoming large ion. Thus, qualitatively fused-salt behavior is similar to that of aqueous electrolytes and the selectivity sequence would depend upon the relative magnitudes of the electrostatic and fused-salt coordination effects. An example has been provided in section V.B.3 where Yao and Kummer used free energies of formation of the salts to represent coordination effects.

Free energies, whether estimated from theory or obtained from experimentally determined values of the equilibrium constant for exchange, serve as a guide to the extent of exchange. Even if the free energy is unfavorable, an appreciable amount of exchange may still be possible by increasing the concentration of the ingoing ion to large values or removing the outgoing ion by volatilization or precipitation. Elevation of the temperature may also change the free energy in a negative direction, thereby increasing the extent of exchange. This change can be very large in the case of inorganic exchangers since many do not decompose up to fairly high temperatures.

B. Kinetic Factors

The rate-determining step in ion exchange is the counterdiffusion of ions within the solid,[175] provided the concentration of ingoing ions at the surface is high enough and stirring does not allow undue concentrations of the outgoing ions to accumulate at the surface of the exchanger. Under such conditions, referred to as the "infinite solution" condition,[175] the fraction of exchange at time t is given by

$$\frac{F(t)}{F(\infty)} = 1 - \left(\frac{6}{\pi^2} \right) \sum_{n=1}^{\infty} \frac{1}{n^2} e^{-n^- BT} \tag{30}$$

where $B = \pi^2 \bar{D}_i / r^2$. $\bar{D}_i$ is the chemical interdiffusion coefficient of the exchanging ions, r is the radius of the exchanger particles (assumed to be spherical), and $F(\infty)$ is the maximum extent of exchange as given by the thermodynamic factors discussed in section VII.A. A small particle size and large interdiffusion coefficient favor rapid exchange. England et al.[37] have calculated the times required to achieve $F(t)/F(\infty) = 0.95$ for spherical particles of 100 μm and a range of $\bar{D}_i$ values. These are collected in Table 7. It is seen that facile exchange requires diffusion coefficients of the order of 10^{-5}–10^{-9} cm^2/s. However, even with diffusion coefficients of 10^{-12} cm^2/s, rapid exchange can occur if the

particles are small enough.[164] All diffusion processes require an activation energy, E_a, to overcome the barrier to diffusion. The magnitude of the barrier may be obtained by determining D_i as a function of temperature since

$$D_i = D_0 \exp(-\Delta E_a / kt) \tag{31}$$

In ion exchange ΔE_a is the energy required for mixed-ion or interion diffusion to occur. Diffusion coefficients are often determined by self-diffusion processes. Use of a single diffusion coefficient does not introduce a large error if the two ions have approximately similar values of D_i. However, if they do not, the error can be quite large as seen from the usual expression for the average value of the interdiffusion coefficient for ion exchange (eq 32)[175]

$$\bar{D}_{AB} = \frac{D_A D_B (Z_A + Z_B)}{Z_A D_A + Z_B D_B} \tag{32}$$

where D_A and D_B are self-diffusion coefficients and Z_A and Z_B are the respective charges on the ions. During an ion exchange reaction the concentration of the two species within the exchanger varies, which causes $\bar{D}_{AB}$ to change according to the expression

$$\overline{\overline{D_{AB}}} = \frac{D_A D_B (Z_A^2 C_A + Z_B^2 C_B)}{Z^2 C_A D_A + Z_B^2 C_B D_B} \tag{33}$$

The above equation appears to hold not only for organic resins but for inorganics where exchange is accompanied by complete solid solution formation. This is the case for amorphous exchangers such as particle hydrates. However, when exchange is accompanied by a phase change, vacancy formation, or in tight structures where interdiffusion is not possible, it is not altogether clear that the above description of kinetic factors is applicable. Furthermore, single-ion transport and ion exchange in such solids may proceed by different mechanisms.[247] More detailed studies of both ion exchange and conduction as a function of structural changes are required. Factors such as those described by England et al. need to be considered.

C. Conclusions

We have tried to show in this review that ion exchange is a widespread phenomenon in inorganic chemistry. New compounds which exhibit ion exchange behavior are being synthesized at a rapid rate. In addition, tight three-dimensional frameworks may be induced to exchange cations at elevated temperatures. These phenomena may be used to synthesize new compounds and to design materials for conduction and ion transport devices such as sensors, fuel cells, and thermoelectric batteries. Ion exchange processes may also prove useful in catalyst development and preparation of crystals with interesting optical properties. A better understanding of diffusion mechanisms as related to ion transport and ion exchange is required, as is a coupling of theory with experiment.

References

(1) Clearfield, A. *Inorganic Ion Exchange Materials*; CRC Press: Boca Raton, FL, 1982.
(2) Vesely, V.; Pekarek, V. *Talanta* **1972**, *19*, 219.
(3) Churms, S. C. *S. Afr. Ind. Chem.* **1965**, *26*, 48, 68, 87, 148.
(4) Breck, D. W. *Zeolite Molecular Sieves, Structure, Chemistry and Use*; Wiley-Interscience: New York, 1974; Chapter 7.
(5) Sherry, H. S. In *The Nature of Sea Water*; Goldberg, E. D., Ed.; Dahlem Conference: Berlin, 1975.
(6) Rees, L. V., Ed. *Proceedings of the 5th International Conference on Zeolites*; Heyden: Philadelphia, 1980; pp 273–334.
(7) Fowden, L.; Barrer, R. M.; Tinker, P. B. *Clay Minerals, Their Structure, Behavior and Use*; Royal Society: London, 1984.
(8) Townsend, R. P. *Pure Appl. Chem.* **1986**, *58*, 1359.
(9) Kashimizu, H.; Otsuka, R. *Gypsum Lime* **1986**, *No. 204*, 328.
(10) Thompson, H. S.; Roy, J. *Agric. Soc. Engl.* **1850**, *11*, 68.
(11) Way, J. T.; Roy, J. *Agric. Soc. Engl.* **1850**, *11*, 313; **1852**, *13*, 12.
(12) Lemberg, J. *Z. Dtsch. Geol. Ges.* **1870**, *22*, 355; **1876**, *28*, 519.
(13) Wiegner, G. *J. Landwirtsch.* **1912**, *60*, 111, 197.
(14) Harm, F.; Rumpler, A. *5th Int. Cong. Pure Appl. Chem.* **1903**, 59.
(15) Gans, R. *Lahrb. Preuss. Geol. Landesanstalt (Berlin)* **1905**, *26*, 179; **1906**, *27*, 63.
(16) Adams, B. A.; Holmes, E. L. *J. Soc. Chem. Ind., London* **1935**, *54*, 1T.
(17) Kraus, K. A.; Phillips, H. O. *J. Am. Chem. Soc.* **1956**, *78*, 644.
(18) Kraus, K. A.; Phillips, H. O.; Carlson, T. A.; Johnson, J. S. *2nd U.N. Conf. Peaceful Uses At. Energy, Geneva* **1958**, *28*, 3.
(19) Amphlett, C. B. *2nd U.N. Conf. Peaceful Uses At. Energy, Geneva* **1958**, *28*, 17.
(20) Amphlett, C. B. *Inorganic Ion Exchangers*; Elsevier: Amsterdam, 1964.
(21) Russel, E. R.; Adamson, A. W.; Shubert, J.; Boyd, G. E. U.S. Atomic Energy Commission Report CN-508, 1943.
(22) Gordon, A.; Betler, O. S.; Greenbaum, M.; Marantz, L.; Gral, T.; Maxwell, M. H. *Trans. Am. Soc. Artif. Int. Organs* **1971**, *17*, 253.
(23) Clearfield, A.; Stynes, J. A. *J. Inorg. Nucl. Chem.* **1964**, *26*, 117.
(24) Clearfield, A.; Stynes, J. A. *J. Inorg. Nucl. Chem.* **1969**, *8*, 431.
(25) Troup, J. M.; Clearfield, A. *Inorg. Chem.* **1977**, *16*, 3311.
(26) Albertsson, J.; Oskarsson, A.; Tellgren, R.; Thomas, J. O. *J. Phys. Chem.* **1977**, *81*, 1574.
(27) Clearfield, A.; Duax, W. L.; Medina, A. S.; Smith, G. D.; Thomas, J. R. *J. Phys. Chem.* **1969**, *73*, 3424.
(28) (a) Barrer, R. M. *Proc. Chem. Soc.* **1958**, 99. (b) Barrer, R. M. *Hydrothermal Chemistry of Zeolites*; Academic Press: New York, 1982.
(29) (a) Breck, D. W.; Eversole, W. G.; Milton, R. M. *J. Am. Chem. Soc.* **1956**, *78*, 2338. (b) Breck, D. W.; Eversole, W. G.; Milton, R. M.; Reed, T. B.; Thomas, T. L. *J. Am. Chem. Soc.* **1956**, *78*, 5963.
(30) Mays, R. L.; Pickert, P. E. In *Molecular Sieves*; Society of Chemical Industry: London, 1968; p 112.
(31) (a) Meisel, S. L.; McCullough, J. P.; Lechthaler, C. H.; Weisz, P. B. *CHEMTECH* **1976**, *6*, 86. (b) Chang, C. D.; Silvestri, A. J. *J. Catal.* **1977**, *47*, 249.
(32) Wilson, S. T.; Lok, B. M.; Messina, C. A.; Cannan, T. R.; Flanigen, E. M. *J. Am. Chem. Soc.* **1982**, *104*, 1146.
(33) England, W. A.; Cross, M. G.; Hamnett, A.; Wiseman, P. J.; Goodenough, J. B. *Solid State Ionics* **1980**, *1*, 231.
(34) Reference 1, pp 167–169.
(35) Clearfield, A. *Inorg. Chem.* **1964**, *3*, 146.
(36) Parks, G. A. *Chem. Rev.* **1965**, *65*, 177.
(37) England, W. A.; Goodenough, J. B.; Wiseman, P. J. *J. Solid State Chem.* **1983**, *49*, 289.
(38) Clearfield, A. *Rev. Pure Appl. Chem.* **1964**, *14*, 91.
(39) Clearfield, A.; Nancollas, G. H.; Blessing, R. H. *Ion Exchange and Solvent Extraction*; Marinsky, J. A., Marcus Y., Eds.; Marcel Dekker: New York, 1973.
(40) Fryer, J. R.; Hutchinson, J. L.; Paterson, R. *J. Colloid Interface Sci.* **1970**, *31*, 238.
(41) Conway, B. E.; Bockris, J. O'M.; Lynton, H. *J. Chem. Phys.* **1956**, *24*, 834.
(42) Dzimitrowicz, D. J.; Goodenough, J. B.; Wiseman, P. J. *Mater. Res. Bull.* **1982**, *17*, 971.
(43) Yamaguchi, T.; Tanabe, K. *Mater. Chem. Phys.* **1986**, *16*, 67.
(44) Tauster, S. J.; Fung, S. C.; Baker, R. T.; Horsley, J. A. *Science (Washington, D.C.)* **1981**, *211*, 1221.
(45) Rijnten, H. T. *Zirconia*; Drukkerij Gebr. Janssen: Nijmegen, 1971.
(46) Reference 1, pp 197–199.

(47) Chowdhry, U.; Barkley, J. R.; English, A. D.; Sleight, A. W. *Mater. Res. Bull.* **1982**, *17*, 917.
(48) Donaldson, J. D.; Fuller, M. J. *J. Inorg. Nucl. Chem.* **1968**, *30*, 1083.
(49) Baetsle, L. H.; Huys, D. *J. Inorg. Nucl. Chem.* **1968**, *30*, 639.
(50) Subramanian, M. A.; Aravamudan, G.; Subba Rao, G. V. *Prog. Solid State Chem.* **1983**, *15*, 55.
(51) Abe, M. *J. Inorg. Nucl. Chem.* **1979**, *41*, 85.
(52) Reference 1, pp 246–256.
(53) Hervieu, M.; Michael, C.; Raveau, B. *Bull. Soc. Chim. Fr.* **1971**, *11*, 3939.
(54) Groult, D.; Michel, C.; Raveau, B. *J. Inorg. Nucl. Chem.* **1974**, *36*, 61.
(55) Rice, C. E.; Jackel, J. L. *J. Solid State Chem.* **1982**, *41*, 308.
(56) Jackel, J. L.; Rice, C. E.; Veselka, J. J. *Appl. Phys. Lett.* **1982**, *41*, 607.
(57) Rice, C. E.; Jackel, J. L. *Mater. Res. Bull.* **1984**, *19*, 591.
(58) Rice, C. E. *J. Solid State Chem.* **1986**, *64*, 188.
(59) Izumi, F.f; Kodama, H. *Z. Anorg. Allg. Chem.* **1978**, *441*, 196.
(60) Bockris, J. O'M.; Reddy, A. K. N. *Modern Electrochemistry*; Plenum Press: New York, 1960; Vol. 1, Chapter 5.
(61) Slade, R. C. T.; Cross, M. G.; England, W. A. *Solid State Ionics* **1982**, *6*, 225.
(62) Ghosh, B. *J. Chem. Soc.* **1926**, 2605.
(63) Kozawa, A. *J. Electrochem. Soc.* **1959**, *106*, 79, 552.
(64) Balenvski, L.; Brenet, J.; Coeffier, G.; Lancon, P. *C. R. Acad. Sci. (Paris)* **1965**, *260*, 106.
(65) Brenet, J. *Chimia* **1969**, *23*, 44.
(66) Leonteva, G. V.; Volkhin, V. V. *Izv. Akad. Nauk. SSSR, Neorg. Mater.* **1968**, *4*, 728; **1969**, *5*, 1224.
(67) Tsuji, M.; Abe, M. *Solv. Extr. Ion Exchange* **1984**, *3*, 30.
(68) Shen, X.-M.; Clearfield, A. *J. Solid State Chem.* **1986**, *64*, 270.
(69) Giovanoli, R.; Stähle, E.; Feitknecht, W. *Helv. Chim. Acta* **1970**, *53*, 209.
(70) Giovanoli, R. *Chimia* **1969**, *23*, 470.
(71) Byström, A.; Byström, A. M. *Acta Crystallogr.* **1950**, *3*, 146; **1951**, *4*, 469.
(72) Wadsley, A. D. *Acta Crystallogr.* **1953**, *6*, 433.
(73) Parant, J.-P.; Olazcuaga, R.; Devalette, M.; Fouassier, C.; Hagenmuller, P. *J. Solid State Chem.* **1971**, *3*, 1.
(74) Wadsley, A. D. *J. Am. Chem. Soc.* **1950**, *72*, 1781.
(75) Wadsley, A. D. *Acta Crystallogr.* **1955**, *8*, 165.
(76) Mathieson, A. McL.; Wadsley, A. D. *Am. Minerol.* **1950**, *35*, 99.
(77) Buser, W.; Graf, P.; Feitknecht, W. *Helv. Chim. Acta* **1954**, *37*, 2322.
(78) Buser, W.; Graf, P. *Helv. Chim. Acta* **1955**, *38*, 810.
(79) Feitknecht, W.; Buser, W. *Z. Elektrochem.* **1956**, *60*, 789.
(80) Thery, J.; Buancon, D.; Collongues, R. *C. R. Acad. Sci. (Paris)* **1961**, *252*, 1475.
(81) Thilo, E.; Geissner, W. *Z. Anorg. Chem.* **1966**, *345*, 151.
(82) Geissner, W. *Z. Anorg. Chem.* **1967**, *352*, 145.
(83) Shannon, R. D.; Rogers, D. B.; Prewitt, C. T. *Inorg. Chem.* **1971**, *10*, 713, 719.
(84) Joubert, J. C.; Durif, A. *Bull. Soc. Fr. Miner. Cristallogr.* **1964**, *87*, 517.
(85) Joubert, J. C. *Bull. Soc. Fr. Miner. Cristallogr.* **1967**, *90*, 598.
(86) Hunter, J. C. *Solid State Chem.* **1970**, *39*, 142.
(87) Milonjić, S. K.; Kopecni, M. M.; Ilić, Z. E. *J. Radioanal. Chem.* **1983**, *78*, 15.
(88) Harding, K. In *Inorganic Ion Exchangers and Adsorbents for Chemical Processing in the Nuclear Fuel Cycle* (IAEA-TEC-DOC-337); International Atomic Energy Agency: Vienna, 1985; pp 97–112.
(89) Bouaziz, R.; Mayer, M. *C. R. Acad. Sci. Paris, Ser. C* **1971**, *272*, 1874.
(90) Wefers, K. *Naturwissenschaften* **1967**, *54*, 19.
(91) Andersson, S.; Wadsley, A. D. *Acta Crystallogr.* **1961**, *14*, 1245.
(92) Dion, M.; Piffard, Y.; Tournoux, M. *J. Inorg. Nucl. Chem.* **1978**, *40*, 917.
(93) Beloyev, E. K.; Safiullin, N. Sh.; Panasenko, N. M. *Inorg. Mater.* **1968**, *4*, 78.
(94) Andersson, S.; Wadsley, A. D. *Acta Crystallogr.* **1962**, *15*, 194.
(95) Wadsley, A. D.; Mumme, W. G. *Acta Crystallogr., Sect. B* **1968**, *B24*, 392.
(96) Watanabe, M.; Bando, Y.; Tsutsumi, M. *J. Solid State Chem.* **1979**, *28*, 397.
(97) Marchand, R.; Brohan, L.; M'Bedi, R.; Tournoux, M. *Mater. Res. Bull.* **1980**, *15*, 1129.
(98) Olazcuaga, R.; Reau, J.-M.; Devalette, M.; Le Flem, G.; Hagenmuller, P. *J. Solid State Chem.* **1975**, *13*, 275.
(99) Bouaziz, R.; Mayer, M. *C. R. Acad. Sci. Paris, Ser. C* **1971**, *272*, 1773.
(100) Werthmann, R.; Hoppe, R. *Z. Anorg. Allg. Chem.* **1984**, *519*, 117.
(101) Izawa, H.; Kikkawa, S.; Koizumi, M. *J. Phys. Chem.* **1982**, *86*, 5023.

(102) Izawa, H.; Kikkawa, S.; Koizumi, M. *J. Solid State Chem.* **1985**, *60*, 264.
(103) Sasaki, T.; Komatsu, Y.; Fujiki, Y. *Solv. Extr. Ion Exchange* **1983**, *1*, 775.
(104) Sasaki, T.; Watanabe, M.; Komatsu, Yu.; Fujiki, Y. *Inorg. Chem.* **1985**, *24*, 2265.
(105) Sasaki, T.; Watanabe, M.; Fujiki, Y. *Sep. Sci. Technol.* **1983**, *18*, 49.
(106) Izawa, H.; Kikkawa, S.; Koizumi, M. *Polyhedron* **1983**, *2*, 741.
(107) Kikkawa, S.; Yasuda, F.; Koizumi, M. *Mater. Res. Bull.* **1985**, *20*, 1221.
(108) Lynch, R. W.; Dosch, R. G.; Kenna, B. T.; Johnstone, J. K.; Nowak, E. J. in *IAEA-SM-207/75*; International Atomic Energy Agency: Vienna, 1975; p 361.
(109) Clearfield, A.; Lehto, J. *J. Solid State Chem.*, in press.
(110) Bursill, L. A.; Kwiatkowski, J. *J. Solid State Chem.* **1984**, *52*, 45.
(111) Grzinic, G.; Bursill, L. A.; Smith, D. J. *J. Solid State Chem.* **1983**, *47*, 151.
(112) Lehto, J.; Meittinen, J. In *Inorganic Ion Exchangers and Adsorbents for Chemical Processing in the Nuclear Fuel Cycle* (IAEA-TEC-DOC-337); International Atomic Energy Agency: Vienna, 1985; pp 9–17.
(113) Lehto, J.; Clearfield, A. *Radioanal. Chem.* **1987**, *118*, 1.
(114) Raveau, B. *Rev. Chim. Miner.* **1984**, *21*, 391.
(115) Rebbah, H.; Desgardin, G.; Raveau, B. *Mater. Res. Bull.* **1979**, *14*, 1125.
(116) Rebbah, H.; Desgardin, G.; Raveau, B. *J. Solid State Chem.* **1980**, *31*, 321.
(117) Hervieu, M.; Raveau, B. *J. Solid State Chem.* **1980**, *32*, 161.
(118) Hervieu, M.; Rebbah, H.; Desgardin, G.; Raveau, B. *J. Solid State Chem.* **1980**, *35*, 200.
(119) Wadsley, A. D. *Acta Crystallogr.* **1964**, *17*, 623.
(120) Rebbah, H.; Borel, M.-M.; Bernard, M.; Raveau, B. *Rev. Chim. Miner.* **1981**, *18*, 109.
(121) Rebbah, H.; Borel, M.-M.; Raveau, B. *Mater. Res. Bull.* **1980**, *15*, 317.
(122) Grandin, A.; Borel, M.-M.; Raveau, B. *J. Solid State Chem.* **1985**, *60*, 366.
(123) Lal, M.; Howe, A. T. *J. Solid State Chem.* **1984**, *51*, 335.
(124) Groult, D.; Mercey, C.; Raveau, B. *J. Solid State Chem.* **1980**, *32*, 289.
(125) Byström, A.; Byström, A. M. *Acta Crystallogr.* **1950**, *3*, 146.
(126) Wadsley, A. D.; Andersson, S. *Nature (London)* **1961**, *192*, 551.
(127) Reid, A. F.; Watts, J. A. *J. Solid State Chem.* **1970**, *1*, 310.
(128) Verbaere, A.; Dion, M.; Tournoux, M. *Rev. Chim. Miner.* **1975**, *12*, 156.
(129) Reid, A. F.; Mumme, W. G.; Wadsley, A. D. *Acta Crystallogr., Sect. B* **1968**, *B24*, 1228.
(130) England, W. A.; Birkett, J. E.; Goodenough, J. B. *J. Solid State Chem.* **1983**, *49*, 300.
(131) Dion, M.; Ganne, M.; Tournoux, M. *Rev. Chim. Miner.* **1986**, *23*, 61.
(132) Dion, M.; Ganne, M.; Tournoux, M.; Ravez, J. *Rev. Chim. Miner.* **1984**, *21*, 92.
(133) Dion, M.; Ganne, M.; Tournoux, M. *Mater. Res. Bull.* **1981**, *16*, 1429.
(134) Ruddlesden, S. N.; Popper, P. *Acta Crystallogr.* **1957**, *10*, 538; **1958**, *11*, 54.
(135) Jacobsen, A. J.; Johnson, J. W.; Lewandowski, J. T. *Inorg. Chem.* **1985**, *24*, 3727.
(136) Jacobson, A. J.; Johnson, J. W.; Lewandoski, J. T. *J. Less-Common Met.* **1986**, *111*, 137.
(137) Jacobson, A. J.; Johnson, J. W.; Lewandowski, J. T., private communication.
(138) Gopalakrishna, J.; Vasudeva, B. *Mater. Res. Bull.* **1987**, *22*, 413.
(139) Michel, C.; Guyomarc'h, A.; Raveau, B. *J. Solid State Chem.* **1977**, *22*, 393.
(140) Michel, C.; Guyomarc'h, A.; Raveau, B. *J. Solid State Chem.* **1978**, *25*, 251.
(141) Desgardin, G.; Robert, C.; Groult, D.; Raveau, B. *J. Solid State Chem.* **1977**, *22*, 101.
(142) Gatehouse, B. M. *J. Solid State Chem.* **1977**, *22*, 404.
(143) Clearfield, A.; Troup, J. M. *J. Phys. Chem.* **1970**, *74*, 2578.
(144) Clearfield, A.; Saldarriaga-Molina, C. H.; Buckley, R. H. *Proceedings of the 3rd International Conference on Molecular Sieves*; Uytterhoeven, J. B., Ed.; University of Leuven Press: Leuven, Belgium, 1973; p 241.
(145) Clearfield, A. *Annu. Rev. Mater. Sci.* **1984**, *14*, 205.
(146) Clearfield, A.; Jahangir, L. M. In *Recent Developments in Separation Science*; Navratil, J. D., Ed.; CRC Press: Boca Raton, FL, 1984.
(147) Clearfield, A.; Thakur, D. S. *Appl. Catal.* **1986**, *26*, 1.
(148) Alberti, G. *Acc. Chem. Res.* **1978**, *11*, 163.
(149) Alberti, G.; Casciola, M.; Costantino, U. *J. Membr. Sci.* **1983**, *16*, 137.
(150) Clearfield, A.; Pack, S. P. *J. Inorg. Nucl. Chem.* **1974**, *37*, 1283.

(151) Tindwa, R. M. Ph.D. Dissertation, Texas A&M University, May 1979.
(152) Hagman, L. O.; Kierkegaard, P. *Acta Chem. Scand.* **1968**, *12*, 1822.
(153) Clearfield, A.; Jirustithipong, P.; Cotman, R. N.; Pack, S. P. *Mater. Res. Bull.* **1980**, *15*, 1603.
(154) Clearfield, A.; Guerra, R.; Oskarsson, Å.; Subramanian, M. A.; Wang, W. *Mater. Res. Bull.* **1983**, *18*, 1561.
(155) Milne, S. J.; West, A. R. *Solid State Ionics* **1983**, *9/10*, 865.
(156) Milne, S. J.; Gard, J. A.; West, A. R. *Mater. Res. Bull.* **1985**, *20*, 557.
(157) Clearfield, A.; Pack, S. P.; Troup, J. M. *J. Inorg. Nucl. Chem.* **1977**, *39*, 1437.
(158) Clearfield, A.; Pack, S. P. *J. Inorg. Nucl. Chem.* **1980**, *42*, 771.
(159) Clearfield, A.; Pack, S. P. *Mater. Res. Bull.* **1983**, *18*, 1343.
(160) Hong, H. Y.-P. *Mater. Res. Bull.* **1976**, *11*, 173.
(161) Goodenough, J. B.; Hong, H. Y.-P.; Kafalas, J. A. *Mater. Res. Bull.* **1976**, *11*, 204.
(162) Chernorukov, N. G.; Korshunov, I. A.; Prokofeva, T. V. *Sov. Phys.—Crystallogr. (Engl. Transl.)* **1978**, *23*, 475.
(163) Clearfield, A.; Jirustithipong, P. In *Fast Ion Transport in Solids*; Vashista, P., Mundy, J. N., Shenoy, G. K., Eds.; Elsevier-North Holland: New York, 1979; Vol. 1, p 153.
(164) Harvie, S. J.; Nancollas, G. H. *J. Inorg. Nucl. Chem.* **1968**, *30*, 273.
(165) Alberti, G.; Allulli, S.; Cardini, G. *J. Chromatogr.* **1969**, *45*, 298.
(166) Allulli, S.; LaGinestra, A.; Tomassini, N. *J. Inorg. Nucl. Chem.* **1974**, *36*, 3839.
(167) Piffard, Y.; Oyetola, S.; Courant, S.; Lachgar, A. *J. Solid State Chem.* **1985**, *60*, 209.
(168) Piffard, Y.; Verbaere, A.; Oyetola, S.; Deniard-Courant, S.; Tournoux, M., private communication.
(169) Chernorukov, N. G.; Egarov, N. P.; Galanova, T. A. *Izv. Akad. Nauk. SSSR, Neorg. Mater.* **1981**, *17*, 328.
(170) Chernorukov, N. G.; Sharova, T. V.; Kryukova, A. I.; Korshunov, I. A. *Russ. J. Inorg. Chem. (Engl. Transl.)* **1985**, *30*, 665.
(171) Beneke, K.; Lagaly, G. *Inorg. Chem.* **1983**, *22*, 1503.
(172) Chernorukov, N. G.; Egarov, N. P.; Kutsepin, V. F. *Russ. J. Inorg. Chem. (Engl. Transl.)* **1979**, *24*, 987.
(173) Piffard, Y.; Verbaere, A.; Lachgar, A.; Deniard-Courant, S.; Tournoux, M. *Rev. Chim. Miner.* **1986**, *23*, 766.
(174) Collongues, R.; Gourier, D.; Kahn, A.; Boilot, J. P.; Colomban, Ph.; Wicker, A. *J. Phys. Chem. Solids* **1984**, *45*, 981.
(175) Helfferich, F. *Ion Exchange*; McGraw-Hill: New York, 1962.
(176) Sizova, R. G.; Voronkov, A. A.; Shumyatskaya, N. G.; Ilyukhin, V. V.; Belov, N. V. *Sov. Phys. Dokl.* **1983**, *17*, 618.
(177) Weunsch, B. J.; Schioler, L. J.; Prince, E. *Proceedings of the Conference on High Temperature Solid Oxide Electrolytes*; Brookhaven National Laboratory, Aug 16–17, 1983; Vol. III, p 59.
(178) Hong, H. Y.-P. *Mater. Res. Bull.* **1978**, *13*, 117.
(179) Subramanian, M. A.; Subramanian, R.; Clearfield, A. *Solid State Ionics* **1986**, *18/19*, 562.
(180) Alberti, G. Reference 1, Chapter 2.
(181) Bell, H. F.; Sayer, M. *The Development of Ceramic Proton Conductors*; Canada Center for Mineral and Energy Technology, DSS File No. 01SU.23440-1-9105, 1983.
(182) Nagai, M.; Nishino, T.; Kanazawa, T. *Solid State Ionics* **1986**, *18/19*, 964.
(183) Eisenman, G. *Biophys. J. Suppl.* **1962**, *2*, 259.
(184) Shannon, R. D.; Taylor, B. E.; English, A. D.; Berzins, T. *Elecrochim. Acta* **1977**, *22*, 783.
(185) Cava, R. J.; Vogel, E. M.; Johnson, D. W., Jr. *J. Am. Ceram. Soc.* **1982**, *65*, C157.
(186) Hong, H. Y.-P. In *Fast Ion Transport in Solids*; Vashista, P., Mundy, J. N., Shenoy, G. D., Eds.; Elsevier-North Holland: New York, 1979.
(187) Peters, C. R.; Bettman, M.; Moore, W.; Glick, M. D. *Acta Crystallogr., Sect. B* **1971**, *B27*, 1826.
(188) Boilot, J. P.; Colomban, Ph.; Collin, G.; Comes, R. *J. Phys. Chem. Solids* **1980**, *41*, 47.
(189) Newsam, J. M.; Tolfield, B. C. *J. Phys. Chem. Solid State Phys.* **1981**, *14*, 1545.
(190) Wang, J. C.; Gaffari, M.; Choi, S. *J. Chem. Phys.* **1975**, *63*, 772.
(191) Bates, J. B.; Wang, J.-C.; Dudney, N. *J. Phys. Today* **1982**, 46.
(192) Boilot, J. P.; Collin, G.; Colomban, Ph.; Comes, R. *Phys. Rev. B* **1980**, *22*, 5912.
(193) Toropov, N. A.; Stukalova, M. M. *C. R. Acad. Sci. URSS* **1939**, *24*, 459.
(194) Yao, Y.-F. Y.; Kummer, J. T. *J. Inorg. Nucl. Chem.* **1967**, *29*, 2453.
(195) Foster, L. M.; Anderson, M. P.; Chandrashekhar, G. V.; Burns, G.; Bradford, R. B. *J. Chem. Phys.* **1981**, *75*, 2412.
(196) Farrington, G. C.; Dunn, B. *Solid State Ionics* **1982**, *7*, 267.
(197) Thomas, J. O.; Alden, M.; Farrington, G. C. *Solid State Ionics* **1983**, *9/10*, 301.

(198) Alden, M.; Thomas, J. O.; Farrington, G. C. *Acta Crystallogr., Sect. C* **1984**, *C40*, 1763; *Acta Crystallogr., Sect. B* **1984**, *B40*, 208.
(199) Boilot, J. P.; Colomban, Ph.; Lee, M. R.; Collin, G.; Comes, R. *Solid State Ionics* **1983**, *9/10*, 315.
(200) Farrington, G. C.; Dunn, B.; Thomas, J. O. *Appl. Phys.* **1983**, *A32*, 151.
(201) Dunn, B.; Farrington, G. C. *Solid State Ionics* **1983**, *9/10*, 223.
(202) Dunn, B.; Farrington, G. C. *Solid State Ionics* **1986**, *18/19*, 31.
(203) Carrillo-Cabrera, W.; Thomas, J. O.; Farrington, G. C. *Solid State Ionics* **1983**, *9/10*, 245.
(204) Pechenik, A.; Whitmore, D. H.; Ratner, M. A. *J. Solid State Chem.* **1985**, *58*, 103.
(205) Glasser, L. *Chem. Rev.* **1975**, *75*, 21.
(206) Bates, J. B., Farrington, G. C., Eds.; *Proceedings of the International Conference on Fast Ion Transport in Solids*; North-Holland Publishing Co.: Amsterdam, 1981.
(207) (a) Kleitz, M., Sapoval, B., Ravaine, D., Eds. *Proceedings of the 4th International Conference on Solid State Ionics, Grenoble France*; North-Holland Publishing Co.: Amsterdam, 1983. (b) Boyce, J. B., DeJonghe, L. C., Huggins, R. A., Eds. *Solid State Ionics—85, Proceedings of the 5th International Conference, Lake Tahoe, CA*; North-Holland Publishing Co.: Amsterdam, 1985.
(208) Poulsen, F. W., Hessel Andersen, N., Clausen, K., Kaarup, S. S., Sørensen, O. T., Eds. *Transport–Structure Relations in Fast Ion and Mixed Conductors, Proceedings of the 6th RISØ International Symposium*; RISØ National Laboratory: Roskilde, Denmark, 1985.
(209) Goodenough, J. B., Jensen, J., Potier, A., Eds. *Solid State Protonic Conductors, III, for Fuel Cells and Sensors*; Odense University Press: 1985.
(210) Huggins, R. A. In *Materials for Advanced Batteries, Proceedings of NATO Symposium on Materials for Advanced Batteries, Aussois, France, 1979*; Murphy, D. W., Broadhead, J., Steele, B. C. H., Eds.; Plenum Press: New York, 1980.
(211) Kreuer, K. D.; Rabenau, A.; Weppner, W. *Angew. Chem., Int. Ed. Engl.* **1982**, *21*, 208.
(212) Alberti, G.; Casciola, M.; Costantino, U.; Levi, G.; Riccardi, G. *J. Inorg. Nucl. Chem.* **1978**, *40*, 533.
(213) Alberti, G.; Casciola, M.; Costantino, U.; Levi, G. *J. Membr. Sci.* **1978**, *3*, 179.
(214) Alberti, G.; Casciola, M.; Costantino, U.; Radi, R. *Gazz. Chim. Ital.* **1979**, *109*, 421.
(215) Clearfield, A.; Berman, J. R. *J. Inorg. Nucl. Chem.* **1981**, *43*, 2141.
(216) Jerus, P.; Clearfield, A. *Solid State Ionics* **1982**, *6*, 79.
(217) Alberti, G.; Casciola, M.; Costantino, U.; Leonardi, M. *Solid State Ionics* **1984**, *14*, 289.
(218) Childs, P. E.; Howe, A. T.; Shilton, M. G. *J. Solid State Chem.* **1980**, *34*, 341.
(219) Howe, A. T.; Sheffield, S. H.; Childs, P. E.; Shilton, M. G. *Thin Solid Films* **1980**, *67*, 365.
(220) Lundsgaard, J. S.; Malling, J.; Birchall, M. L. S. *Solid State Ionics* **1982**, *7*, 53.
(221) Childs, P. E.; Halstead, T. K.; Howe, A. T.; Shilton, M. G. *Mater. Res. Bull.* **1978**, *13*, 609.
(222) Bernard, L.; Wright, A. F.; Fender, B. E.; Howe, A. T. *Solid State Ionics* **1981**, *5*, 459.
(223) Gordon, R. E.; Strange, J. H.; Halstead, T. K. *Solid State Commun.* **1979**, *31*, 995.
(224) Tsai, Y.-T.; Halperin, W. P.; Whitmore, D. H. *J. Solid State Chem.* **1983**, *50*, 263.
(225) Pekarek, V.; Benesova, M. *J. Inorg. Nucl. Chem.* **1964**, *26*, 1743.
(226) Pekarek, V.; Vesely, V. *J. Inorg. Nucl. Chem.* **1965**, *27*, 1151.
(227) Vesely, V.; Pekarek, V.; Abbrent, M. *J. Inorg. Nucl. Chem.* **1965**, *27*, 1159.
(228) Tofield, B. C. In *Intercalation Chemistry*; Whittingham, M. S., Jacobson, A. J., Eds.; Academic Press: New York, 1982; Chapter 6.
(229) Frase, K. G.; Farrington, G. C.; Thomas, J. O. *Annu. Rev. Mater. Sci.* **1984**, *14*, 279.
(230) Clearfield, A.; Roberts, B. D.; Subramanian, M. A. *Mater. Res. Bull.* **1984**, *19*, 219.
(231) Ono, A. *J. Mater. Sci.* **1984**, *19*, 2691.
(232) Subramanian, M. A.; Roberts, B. D.; Clearfield, A. *Mater. Res. Bull.* **1984**, *19*, 1471.
(233) Rudolf, P. R.; Subramanian, M. A.; Clearfield, A.; Jorgensen, J. D. *Solid State Ionics* **1985**, *17*, 337.
(234) Nakamura, D.; Kodama, T.; Ogino, I.; Miyake, Y. *Chem. Lett.* **1979**, 17.
(235) Takahashi, T.; Iwahara, H. *Rev. Chim. Mineral.* **1980**, *17*, 243.
(236) Uchica, H.; Maeda, N.; Iwahara, H. *Solid State Ionics* **1983**, *11*, 117.
(237) Lundsgaard, J. S.; Brook, R. J. *J. Mater. Sci.* **1974**, *9*, 2061.
(238) Jensen, J.; McGeehan, P. *Silicates Ind.* **1979**, *9*, 191.
(239) Clearfield, A.; Nguyen, H., work in progress.

(240) Reichle, W. T. *CHEMTECH.* **1986**, 58.
(241) Sissoko, I.; Iyagba, E. T.; Sahai, R.; Biloen, P. *J. Solid State Chem.* **1985**, *60*, 283.
(242) Bish, D. L. *Bull. Mineral.* **1980**, *103*, 170.
(243) Miyata, S.; Kumura, T. *Chem. Lett.* **1978**, 843.
(244) Gaines, G. L.; Thomas, H. C. *J. Chem. Phys.* **1953**, *21*, 714.

(245) Eisenman, G., Ed. *Glass Electrodes for Hydrogen and Other Cations*; Marcel Dekker: New York, 1967.
(246) Clearfield, A.; Day, G. A.; Pack, S. P. *J. Phys. Chem.* **1983**, *87*, 5003.
(247) Constantino, U.; Naszodi, L.; Szirtes, L.; Zsinka, L. *J. Inorg. Nucl. Chem.* **1978**, *40*, 901.